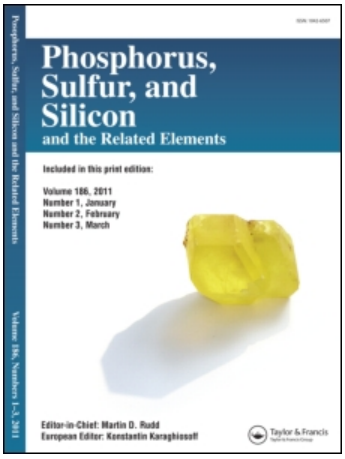

Phosphorus, Sulfur, and Silicon and the Related Elements
Publication details, including instructions for authors and subscription information:
http://www.informaworld.com/smpp/title~content=t713618290

Molecular States of Sulfur Compounds in the Gasphase, in Solution and in Crystals

Hans Bock[a]
[a] Institute of Inorganic Chemistry, University of Frankfurt, Frankfurt (Main), FRG

To cite this Article Bock, Hans(1994) 'Molecular States of Sulfur Compounds in the Gasphase, in Solution and in Crystals', Phosphorus, Sulfur, and Silicon and the Related Elements, 95: 1, 165 — 214
To link to this Article: DOI: 10.1080/10426509408034208
URL: http://dx.doi.org/10.1080/10426509408034208

Phosphorus, Sulfur, and Silicon, 1994, Vol. 93–94, pp. 165–214
Reprints available directly from the publisher
Photocopying permitted by license only

MOLECULAR STATES OF SULFUR COMPOUNDS IN THE GASPHASE, IN SOLUTION AND IN CRYSTALS[1]

HANS BOCK
Institute of Inorganic Chemistry, University of Frankfurt,
Marie Curie-Str. 11, 60439 Frankfurt (Main), FRG

Abstract: The molecular states of selected sulfur compounds are summarized for the first time using the qualitative model approach based on topology, symmetry, effective nuclear potentials as well as electron distribution and supported by quantum chemical calculations to rationalize and to predict structure/energy relations coupled by dynamics. Topics discussed comprise: (i) The gasphase preparation of numerous short-lived sulfur compounds such as $H_2C{=}S$, SN, SSO, HNSO, $HC{\equiv}C\text{-}HC{=}S$ and $H_2C{=}CH\text{-}HC{=}S$, $RP{=}S$ or $RP(=S)_2$) and their characterization by radical cation state fingerprints. (ii) Radical ion generation of sulfur-containing species such as $R_\pi(SR)_n^{\bullet\oplus/\ominus}$, $S_2(CH_2)_3^{\bullet\oplus}$ or $R_2NSSNR_2^{\bullet\oplus}$ in solution by favorable $AlCl_3/H_2CCl_2$ oxidation or metal mirror reduction and their characterization by ESR/ENDOR spectroscopic signal patterns. (iii) Growth of molecular crystals and structure determination of sulfur compounds and their ion salts such as the halogen charge transfer complexes $\{(R_\pi(SR)_n\cdots Hal_2\}$ or the polymorphs of 2,3,7,8-tetramethoxythianthrene and its cyanine-perturbed dication $[M^{\oplus\oplus}][SbCl_6^{\ominus}]_2$. In addition, quantum chemical energy hypersurface calculations are reported to carefully elaborate on rotational dynamics in multi-degree of freedom compounds such as $H_5C_6\text{-}SH$ or $S_2(CH_2)_3$ or reaction pathways such as the isomerisation $XS{=}SX \rightarrow X_2S{=}S$ or the selective thermal fragmentation of $(HC{\equiv}C\text{-}H_2C)_2S$.

I. STARTING POINT: THE MOLECULAR STATE APPROACH TO DESIGN SULFUR COMPOUNDS AND TO RATIONALIZE THEIR PROPERTIES

The structure of a molecule can change considerably as its energy and thus its electron distribution varies within the time-domain of dynamic relaxation. Therefore, the real building blocks of a chemist - as documented for

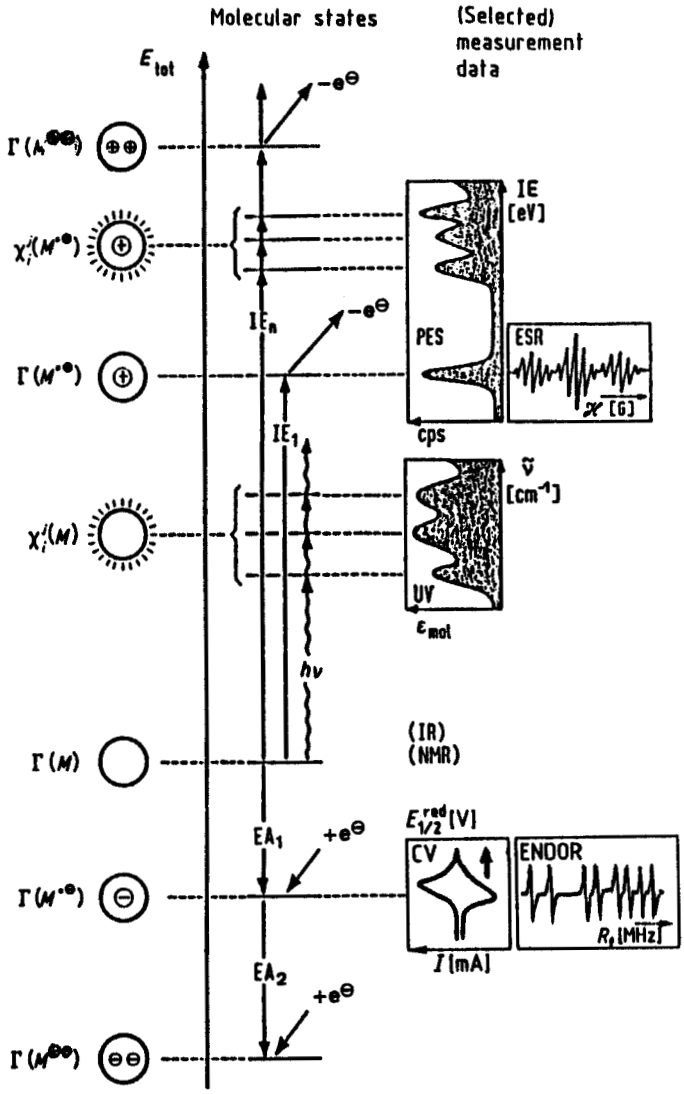

FIGURE 1. Schematic energy scale for electronic ground (Γ) and excited (χ_i^j) states of a neutral molecule M and its radical cation $M^{\bullet\oplus}$ or dication $M^{\oplus\oplus}$ generated by ionization or oxidation and its radical anion $M^{\bullet\ominus}$ and dianion $M^{\ominus\ominus}$ resulting from electron insertion as well as representative measurement methods such as UV, PES, ESR, and ENDOR spectroscopy as well as cyclic voltammetry (CV).

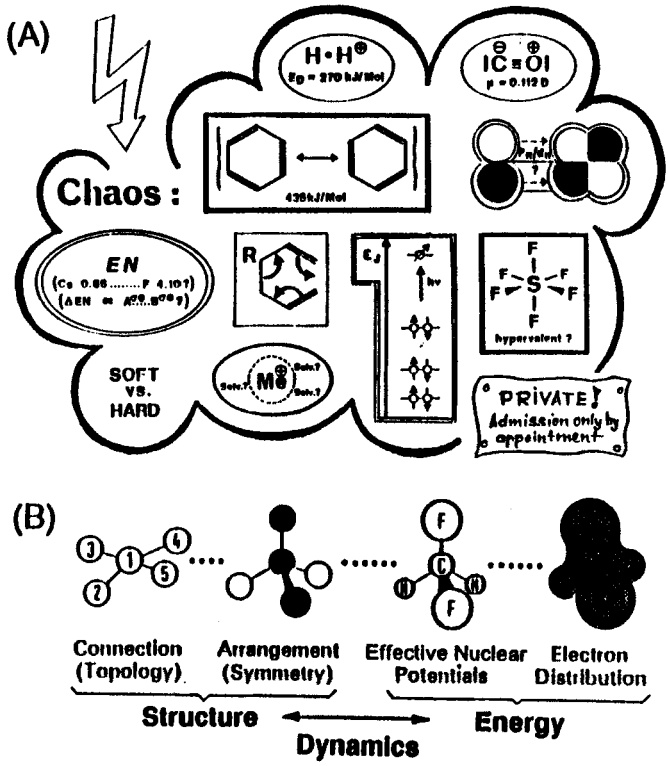

FIGURE 2. Models to rationalize and predict molecular properties (A) far from and (B) close to experimental reality (Figure 1): (A) Selected individual facets based on misleading assumptions of "atoms" in molecules and localized n = 2,4,6 electron bonds (clockwise from high noon): the strong one-electron bond in $H_2^{\bullet\oplus}$, wrong valence bond description of CO as demonstrated by its dipole moment, fictive d-orbitals leading partly to fictive hypervalency, usually insufficient orbital description of excited states, often missing metal ion solvation, fictious concepts of hard vs. soft centers and their electronegativity ("power of an atom in a molecule to attract electrons") and fictious aromaticity as well as bond reshuffle ("if the electron is ever detected by an organic chemist, it will have the shape of a curved arrow", W.E. v. Doehring). (B) Qualitative molecular state approach via topology (two-dimensional), symmetry (three-dimensional), effective nuclear potentials and electron distribution, well-suited for discussion of structure ↔ energy relations coupled by molecular dynamics (cf. text).

example by photochemical synthesis steps or by redox reaction products - are no longer the over 10^7 molecules now known, but increasingly their numerous molecular and molecular ion states[1-7] accessible via various routes of energy transfer as revealed by spectroscopic band or signal patterns, through which the respective compounds may be identified and characterized (Figure 1). In addition to this analytical "ear-marking", such measurements generally provide often unused information on the compounds investigated, which is especially valuable in the planning and evaluation of experiments at a time when at least one chemical publication appears in every one of the 525600 minutes of a 365-day year. Accordingly, the mostly chaotic "private" approaches to rationalize bonding (Figure 2: A) should be replaced by a more rational generalization of experimental data based on connectivity, symmetry, effective nuclear potentials as well as electron distribution and the rather important structure $\leftrightarrow$ energy relations via the inherent molecular dynamics (Figure 2: B). Molecular states and their measurement data can be arranged with respect to both energy [2-4] (Figure 1) and time scales [5].

In general, molecules may be viewed[2] as self-dedicated computers, which in "printing out" measurement data, provide complete i.e., self-consistent and completely correlated solutions of the Schrödinger equation. The question resulting from the rapid development of numerical quantum chemistry software as well as of computer hardware, whether to measure or to calculate, is best answered with reference to how successful and stimulating the combination of the two proves to be. Among the numerous techniques of measurement now available, photoelectron (PE) spectroscopy[2,3] and electron spin resonance (ESR/ENDOR) [2-4] spectroscopy have proven themselves especially informative for preparatively oriented molecular-state investigations (Figure 1). "Vertically" recorded ionization energy patterns i.e., those with a time resolution on the order of 10^{-15} seconds, can be approximately correlated via Koopmans' theorem, $IE^{v}_{n} = -\varepsilon_j^{SCF}$, with the SCF eigenvalues[2] calculated for the neutral molecule M and, therefore, PE spectrometers can thus be looked at as "eigenvalue meters". ESR/ENDOR signal patterns, on the other hand, are recorded "adiabatically" with a considerably smaller time resolution of about 10^{-7} second i.e., long after the onset of molecular dynamics at about 10^{-13} seconds. ESR/ENDOR spectrometers can be considered as "π-eigenfunction-squared meters", since the detected π-spin population ρ^{π}_{μ}

of radical and radical-ion centers can be correlated with the squared orbital coefficient $(c^{\pi})^2$. [2-7] Obviously, the two methods complement each other owing to their different time resolution and allow for example, coupled with quantum-chemical calculations, to determine both the energy and structure changes during one-electron oxidations, $M \rightarrow M^{\bullet\oplus} + e^{\ominus}$.

Molcular crystals contain main group element compounds in their respective ground state close to or even in their global energy minima and with largely "frozen" molecular dynamics.[5-7] Their structure analysis, therefore, provides an advantageous starting point for the discussion of numerous molecular properties and their quantum chemical calculation. Nowadays most of these structures can be predicted either from relevant molecular state measurement data or by approximate energy hypersurface calculations,[5] thereby increasing the hit rate of targeted synthesis efforts and consecutive, often laborious attempts to grow single crystals from aprotic solutions ($c_{H\oplus} < 1$ ppm) under argon. Interactions documented by the crystal structural data, in addition provide static aspects of molecular self-organization.[6,7]

Starting from quantum-chemical precalculations and with extensive preparative efforts, the Frankfurt group[1,6] has carried out numerous investigations of compounds, especially those containing nonmetal elements such as B, C, N, Si, P and S, by using the methods of measurement outlined (Figure 1). For the element sulfur, these investigations are summarized here for the first time and will also include comparison of

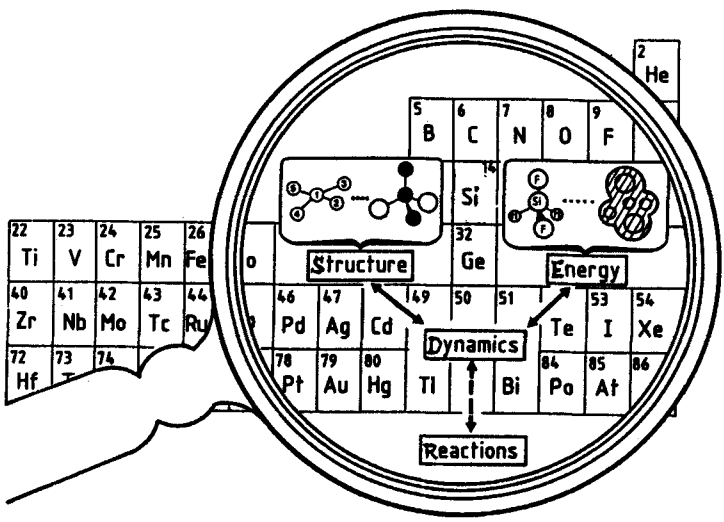

(1)

equivalent states of chemically related molecules[2] in order to recognize additional useful correlations especially those based on first and second order perturbation arguments such as "substituent effects" on "parent systems".[2-5] Let us, therefore, take a "molecular-state magnifying glass" (1) with a special focus on sulfur and examine relations between structure and energy for some selected compounds. Let us begin by discussing the individual components of the qualitative molecular state model (Figure 2: B), which are the connection between the centers, their spatial arrangement, their effective nuclear potentials, and the resulting electron distribution.[2] The inherent rather drastic simplifications, which are, however, supported by quantum chemical calculations, accentuate that each molecular state defined accordingly on changes in its energy and its charge distribution will always provoke structural changes through the inherent molecular dynamics (Figure 2: B). In addition, such a "static background" of structure-energy relationships will throw light on "dynamic phenomena", without which the largely unknown microscopic pathways of chemical reactions, particularly those of medium-sized molecules[8-11] cannot be described.

Altogether hope is expressed that the reader will eventually answer the question "What can the preparative sulfur chemist learn by looking at molecular states?" by "More, presumably, than I have imagined ..."

II. THE QUALITATIVE MOLECULAR STATE MODEL EXEMPLIFIED FOR SELECTED SULFUR COMPOUNDS

Even the predominantly preparative chemist profits considerably, if he looks at his instrumental analysis spectra from the additional point of view that these represent 'molecular state fingerprints'.[2,4,9-11] One example each for the model facets (Figure 2: B) such as topology, symmetry, potentials, electron distribution and dynamics as well as an additional example for the discussion of an reaction pathway will serve to illustrate both the approach and the accessible information.

A. Topology: The Ensemble C_3H_4S

The preparation of reactive organic intermediates by means of thermal decomposition in the gas phase can be optimized advantageously by following the PE spectroscopic "molecular fingerprints" in a flow system:

those of the starting materials will vanish and those of the products emerge. [9-11,13] One of the most favorable leaving groups in the thermal decompositions from allylic compounds is propene[11] and, expectedly, on passing diallyl sulfide under close to unimolecular conditions at 10^{-4} mbar through a tube heated to temperatures above 660 K, propene is readily split off: [13]

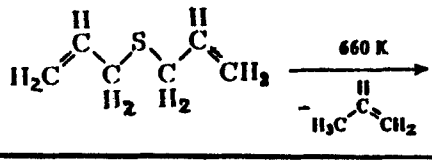

(2)

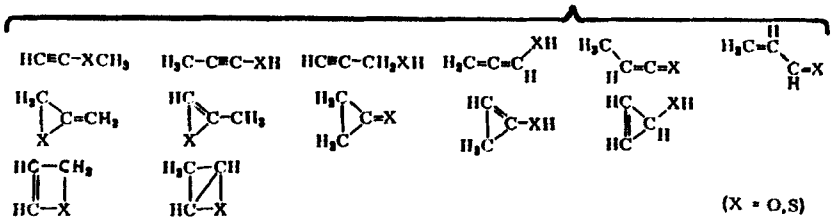

What will be structure of the other thermolysis product with the composition C_3H_4S ? A connectivity computer subroutine,[3] on loading the usual coordination numbers 2 for X = S,O , 2 to 4 for C and 1 for H, yields for the ensemble C_3H_4X six linear chain structures, five containing a three-membered ring and each one a heterocyclobutene and bicyclobutane skeleton (2). Their subsequently calculated MNDO enthalpies of formation yield valence isomer sequences (Figure 3), in which each the compound of topology H_2C=CH-HC=X is predicted to be the most stable one. By cool-trapping, a Diels/Alder dimer mixture can be isolated as a solid and characterized by NMR. On evaporating the slowly polymerizing liquid again while heating the vapor to 670 K oven temperature, the PE spectrum of pure thioacrolein (3) can be recorded.

The PE spectroscopic assignment is easily accomplished by a Koopmans' correlation, $IE_n = -\varepsilon_j^{MNDO}$, with MNDO eigenvalues,[13] according to which the radical ground state $\tilde{X}(^2A')$ with predominant sulfur n_S lone pair contribution is followed by the excited π state $\tilde{A}(^2A'')$ and the second one $\tilde{B}(^2A'')$ at about 12 eV (3). Further conformation is provided by the radical cation state comparison with the iso(valence)electronic acrolein, the PE spectrum of which (3) displays a similar ionization pattern shifted to higher energy due to the increased effective nuclear charge of oxygen relative to sulfur [3] (see chapter II: C).

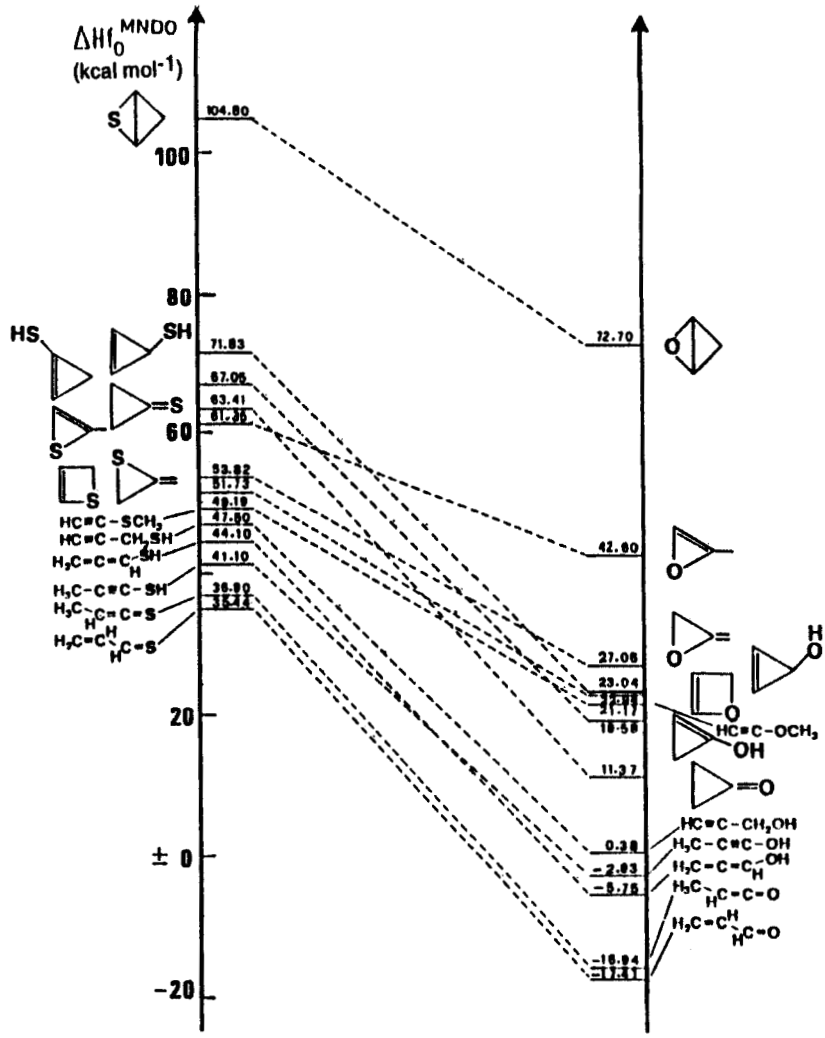

Figure 3 MNDO enthalpies of formation for both the isovalence electronic ensembles C_3H_4S and C_3H_4O according to the topology evaluation of six linear chain structures, five containing a three-membered ring and two with each a cyclobutene and bicyclobutane one (2).

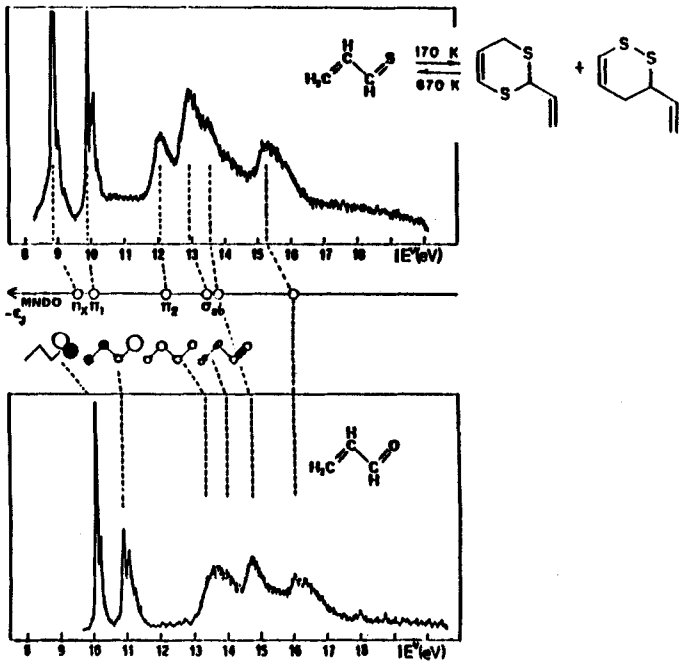

(3)

(4)

Take Home Lesson: Thus, by thermal retrodiene splitting of the Diels/Alder dimer mixture, which can be isolated and steam-distilled, thioacrolein becomes available for preparative use and further investigation e.g. concerning its bioactivity as one of the odor components of garlic.[14] Essential in the optimization of the thermolysis conditions as well as in the assignment of the ionization pattern has been the topology-based evaluation of feasible valence isomers and the subsequent enthalpy selection of thioacrolein (Figure 3) as the thermodynamically most stable valence isomer - a help much appreciated by the experimentalist.

B. Symmetry: The structure of $H_3CS\text{-}C{\equiv}C\text{-}SCH_3$ in the Gasphase

The gasphase thermolysis of bis(methylthio)cyclobutene-1,2-dione at 720 K according to real-time gas analysis by photoelectron (PE) spectroscopy proceeds largely selective by elimination of two CO as energetically favorable leaving molecules ($\Delta H^{o}_{f,273}$ = -110 kJ mol^{-1}) to form bis(methylthio)acetylene.[15] Two preferred conformations are possible with the CS substituent bonds either coplanar (C_{2h}) or perpendicular (C_2) to each other:

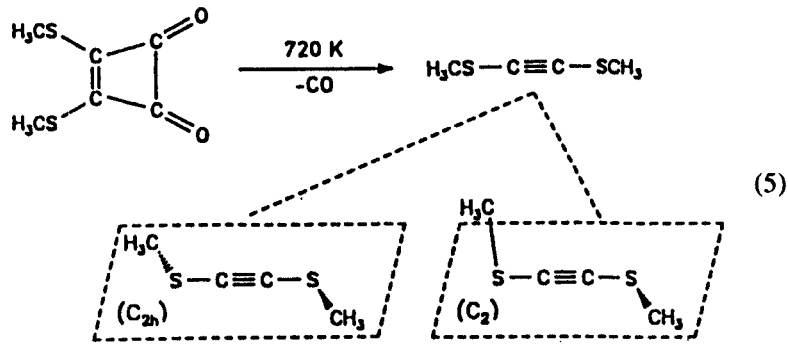

(5)

The two conformers can be characterized and their differences evaluated by calculation of an approximate one-dimensional energy hypersurface (Figure 4), in which only one of the total of (3n - 6) = 30 degrees freedom for the molecule containing n = 12 centers, namely the dihedral angles ω(CS-CC) are considered (Figure 4). [5,15]

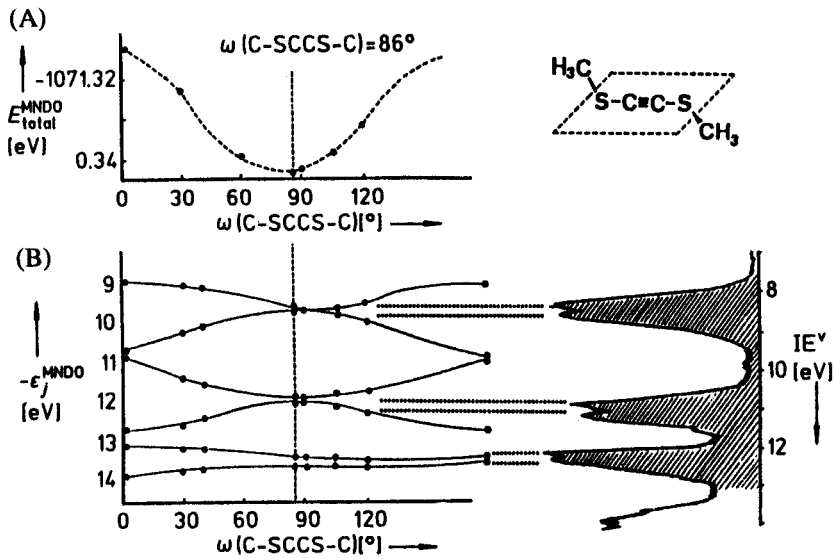

Figure 4. Structural characterization of bis(methylthio)acetylene, generated thermally in the gasphase: (A) One-dimensional total energy hypersurface as a function of its dihedral angles ω(CS-CC) and (B) Koopmans' correlation of the eigenvalue pattern with the six lowest vertical ionization energies, IE^{V}_{n}, determined by PE spectroscopy.

The MNDO potential minimum predicts a dihedral angle of 86°, and the MNDO eigenvalues calculated for the C_2 conformation reproduce via Koopmans' correlation, $-\varepsilon_j^{MNDO} = IE_n^v$, the three double bands observed in the PE spectrum at low energy (Figure 4). An independent structure determination of $H_3CS\text{-}C{\equiv}C\text{-}SCH_3$ by electron diffraction in the gasphase confirms the preferred conformation deduced both from the energy hypersurface minimum and from the correlation of the measured vertical ionization energies with the calculated eigenvalue pattern. The dihedral angle is consistently determined to be 86° [15,16] and the molecular symmetry, therefore, C_2.

Take Home Lesson: In cases of predominant symmetry notation, even gasphase structures can be determined via the pattern of the radical cation states and their irreducible representations - greatly supported by an elegant one-dimensional hypersurface based on the assumption of an highly populated rotational degree of freedom.

C. Effective Nuclear Potentials: H_2S and H_2O

Within the qualitative molecular state model (Figure 2: B),[2] furthermore, potentials have to be defined for the individual centers in such a way that the resulting electron distribution reproduces all important details of molecular structure and other molecular properties, if necessary as changes in energy. For the chemist it is important that such a model permits comparison of experimental data applying to corresponding states of chemically related molecules.[2,3] In general, the distribution or motion of an electron in the time-averaged field of the nuclei and the other electrons of a molecule, can be approximated by molecular orbitals models of varying sophistication. These are especially suitable for discussion of one-electron properties such as the states of radical cations $M^{\bullet\oplus}$ arising on photo-ionization of an electron, $M + h\nu \rightarrow M^{\bullet\oplus} + e^{\ominus}$, within 10^{-15} seconds, i.e. without a structural change relative to the ground state of the neutral molecule. The energy difference on vertical ionization, $\Delta E_{total} = IE^v_n \equiv -\varepsilon_J^{SCF}$, can be correlated via Koopmans' theorem with (one-electron) orbital energies $-\varepsilon_J^{SCF}$ of "Self Consistent Field" quality. An didactically advantageous example are the four states of the triatomic radical cation $HSH^{\bullet\oplus}$ resulting on single valence electron ionization (6). [2]

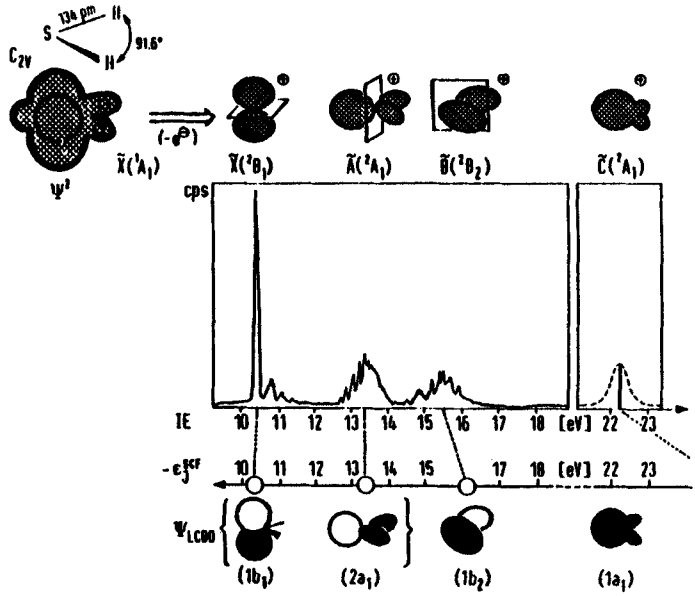

(6)

Ejection of a valence electron from the HSH molecule, which exhibits an almost spherical charge distribution in the ground state, leads to four states of the radical cation $HSH^{\bullet\oplus}$ observable in the PE spectrum. In these states the distribution of the electron hole can be described by calculating the difference electron density between the initial state and the pertinent final state (6): Evidently, often nodal planes result, whose positions relative to the molecular skeleton are reflected by the symmetry classification of the radical cation state.[2] If Koopmans' theorem applies, then the individual states are represented by a set of molecular orbitals Ψ, which can be constructed qualitatively by symmetry-adapted linear combinations of e.g. bond orbitals (6). These molecular wave-functions Ψ_{LCBO} are themselves not experimental observables; however, their squares Ψ^2 can be correlated with experimental electron densities as is obvious from the resulting nodal planes. This will be further substantiated by a PE spectroscopic comparison of the iso(valence)electronic compounds HSH and HOH (Figure 5), which differ primarily in the higher effective nuclear potential of the oxygen center and in the larger HOH angle. Assuming that a radical cation ground state $\tilde{X}(^2B_1)$ scaling is appropriate, the difference in the effective nuclear potentials of S and O centers becomes apparent in the 2.15 eV shift needed to align both PE spectra (Figure 5).

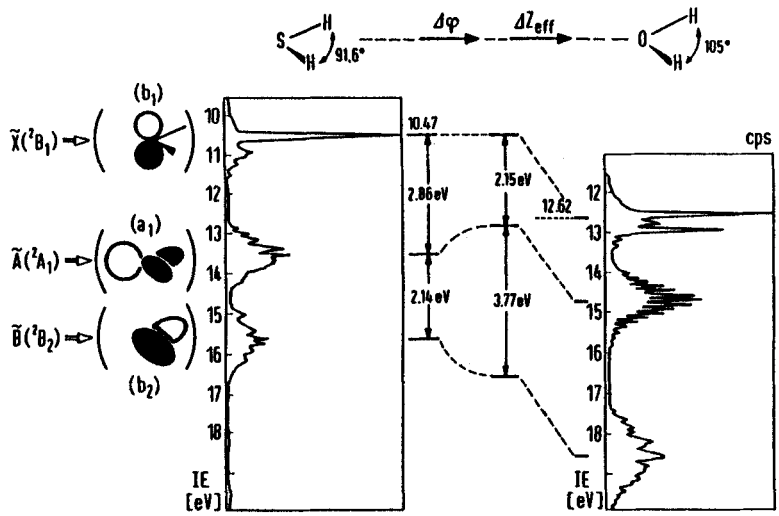

Figure 5 Comparison of the first three radical cation states $\tilde{X}(^2B_1)$, $\tilde{A}(^2A_1)$, and $\tilde{B}(^2B_2)$ of the iso(valence)electronic triatomic molecules HSH and HOH. Attention has to be focussed both on the change of the bond angle $\Delta\varphi$ and the differing effective nuclear charge ΔZ_{eff} of S and O centers. Assuming the first ionization, assigned each to the nonbonding electron pair, to constitute a suitable internal standard, ΔZ_{eff} can be compensated by a relative shift of the PE spectra [2] by 12.62-10.47 = 2.15 eV. The opening of the angle $\Delta\varphi$ can be discussed based on the molecular orbitals (b_1), (a_1), and (b_2) as follows: diminution of the bonding interaction and augmentation of the antibonding interaction in (a_1) raises (destabilizes) this orbital, while diminution of the antibonding interaction in (b_2) lowers (stabilizes) that orbital. The result is an experimental Walsh diagram, which permits comparison of the radical cation states of the chemically related molecules HSH and HOH.

On the 2.15 eV calibration of the HSH and HOH ionization patterns, the angle opening effects becomes clearly recognizable (Figure 5). They had been correctly predicted by Walsh in 1953[17] - ten years before the discovery of PE spectroscopy: $\Delta IE_{1,2}$ decreases and $\Delta IE_{2,3}$ increases as can be rationalized in orbital language by varying bonding or antibonding interactions as denoted by sign equivalence or change in sign and indicative for stabilization or destabilication of the respective radical cation state.

Take Home Lesson: The comparison of $HSH^{\bullet\oplus}$ and $HOH^{\bullet\oplus}$ clearly reveals the effect of different effective nuclear charges at the hetero centers and, in addition, their correlation to ionization potentials i.e. close to experimental reality (Figure 2: A und B). Conversely, the applicability of perturbation arguments to the comparison of molecular states of chemically related compounds furnishes overviews, which often help the preparative chemist tremendously in both the design and rationalisation of his experiments.

D. Electron Distribution: The Cyanine Distortion in 2,3,6,7-Tetramethoxythianthrene Dication

The fascinating (4n + 2)-electron rule for cyclic π systems proposed by E. Hückel [2,18] has stimulated the syntheses of novel molecules and the generation of novel molecular ions with an energetically favorable electron distribution, which in lab jargon are frequently termed "aromatic" (Greek: aromatikos = herbal smelling). Vice versa, deviations from the optimum number of electrons should inflict severe perturbations and, as is known for redox reactions of other organic compounds, result in surprising structural changes.[5] In this respect, 2,3,6,7-tetramethoxythianthrene with 16 π electrons and related to the tricyclic hydrocarbon anthracene with 14 π electrons, is an interesting sulfur model compound, because the "butterfly"-like folding of its skeleton is flattened on single electron-oxidation to its blue radical cation (7). [19]

The 2,3,6,7-tetramethoxythianthrene dication, which can be prepared by oxidation with $SbCl_5$ in H_2CCl_2 under argon and under aprotic conditions ($c_{H\oplus}$ < 1 ppm) and crystallizes in dark-red rhombuses with a metallic luster exhibits an unexpected structure: Despite its 14 π electrons in the three annelated six-membered rings, no fictious "aromatic" character (Figure 2: A) can be detected. Instead, the π molecular skeleton is extended by the methoxy oxygens to include altogether 18 centers, the O-C and C-S bonds are shortened to 132 as well as 170 pm and the ring C-C bonds are elongated to 147 or 145 pm (6). [19] The structure of the dication $M^{\oplus\oplus}$, accordingly consists of two positively charged chains, $H_3CO\text{-}CCC\text{-}S^{\oplus}\text{-}CCC\text{-}OCH_3$, connected by four ring linkages of close to single C-C bond length. This assumption is supported by geometry-optimized MNDO calculations,[19] which reproduce satisfactorily both the structure (e.g. C2-C3 = 148 pm) and the color ($\nu^{exp.}$ = 14100 cm^{-1}, ν^{calcd} = 13700 cm^{-1}) of the dication.

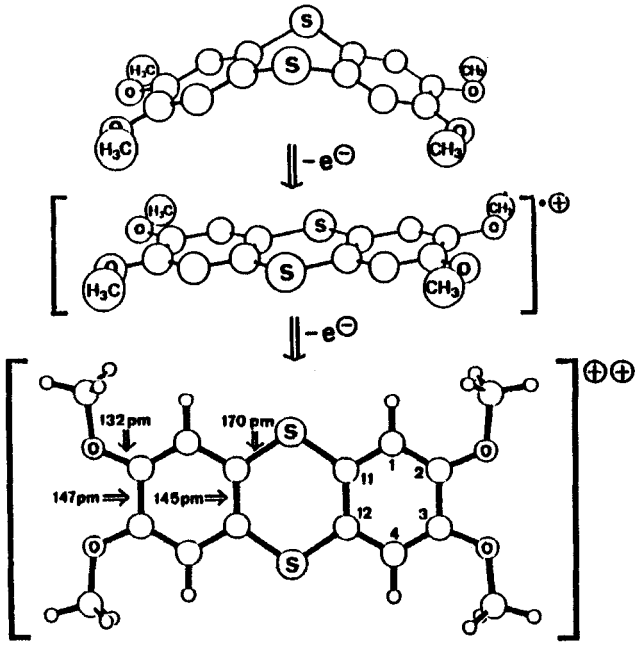

(7)

The charge distributions calculated[19]

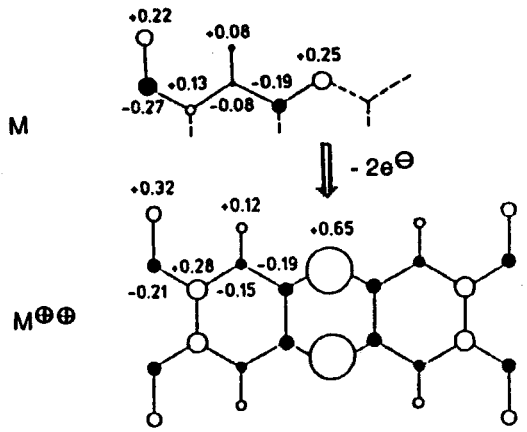

(8)

demonstrate a localization of the positive charges predominantly at the electron-rich sulfur centers and, to a lesser extent, around the methoxy oxygens, which possess the highest effective nuclear charge within the σ skeleton. In addition, the electron densities, which decrease significantly

especially at the outer ring centers, plausibly explains the elongation of the C2-C3 and C11-C12 inner ring bond distances by 7 pm each (7).[19] Altogether, the structural (7) and quantum-chemical (8) data for 2,3,6,7-tetramethoxythianthrene dication can be discussed in terms of the well-tested "cyanine distortion" concept[5] for chain-like π subsystems with an even number of π electrons distributed over an odd number of π centers, which is also responsible for twisted ethylene dications and dianions with a single C-C bond, $R_2C^{\oplus}$-$^{\oplus}CR_2$ and $R_2C^{\ominus}$-$^{\ominus}CR_2$.[5]

Take Home Lesson: In 2,3,6,7-tetramethoxythianthrene dication, experimental structure determination and calculated charge distribution both prove that the formation of two positively charged chains H_3CO-CCC-$S^{\oplus}$-CCC-OCH_3, connected by elongated C-C bonds,[19] wins over an increased cyclic π delocalization in the three annelated six-membered rings. Numerous and partly breath-teaking examples confirm, that the cyanine concept constitutes a general and powerful structure perturbation principle.[5]

E. Molecular Dynamics: Pseudorotation in Dithiolane Radical Cation

The four basic concepts of the qualitative molecular state model (Figure 2: B) - "topological" connections, "spatial" symmetry, effective nuclear potentials and electron distribution within them - have been illustrated by transparent examples such as C_3H_4S isomers (Figure 3), the conformation of H_3CS-C≡C-SCH_3 (Figure 4), gasphase radical cations $HSH^{\bullet\oplus}$ and $HOH^{\bullet\oplus}$ (Figure 5) and the charge/electron distribution within the tetramethoxythianthrene dication (see (7) and (8)).

Molecular dynamics and, more specifically, the predominant population of certain degrees of freedom of the 3N-6 ones in a three-dimensional, N center molecule will be illustrated by the pseudorotation in a five-membered disulfide ring: The radical cation $(H_2C)_3S_2^{\bullet\oplus}$, generated in solution [20] from the neutral compound by using the advantageous single-electron redox system[4,21] $AlCl_3/H_2CCl_2$ exhibits a temperature-dependent ESR signal pattern: [20] At 180 K it consists of a triplet of triplets caused by each two of the adjacent $(CH_2)_2$ hydrogens and after coalescence of each three "inbetween" lines between 200 and 220 K eventually at 270 K of a quintet due to the now equivalent four adjacent $(CH_2)_2$ hydrogens (9).

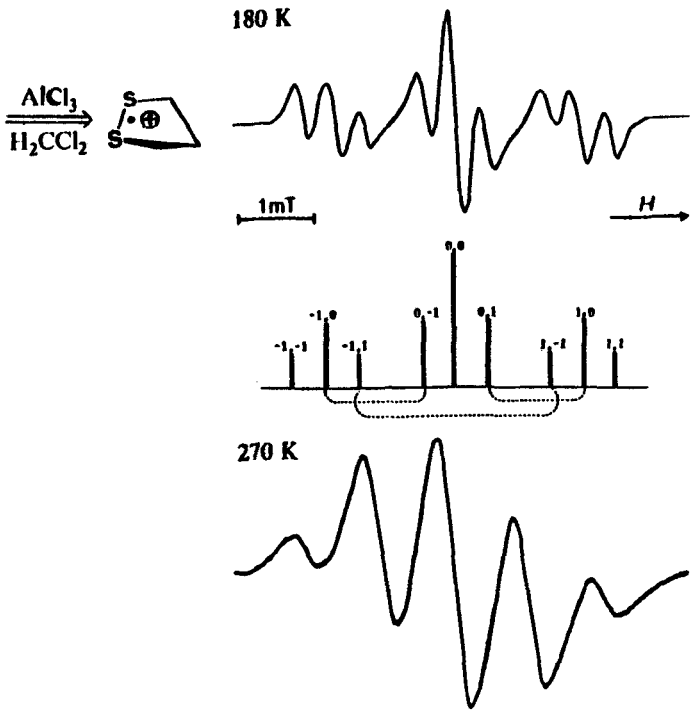

(9)

Via the line broadening (-1,0) → (-1, -1) and the Arrhenius correlation lnk/T, an activation barrier $E_A \approx 8$ kJ mol^{-1} is determined for the equilibration 2 $(CH)_2 \rightarrow (CH_2)_2$. Best discussed in terms of a ring pseudorotation,it can be analyzed by a combination of twisting $\Delta\omega$ around and swing $\Delta\varphi$ through a time-averaged plane of the five-membered ring (Figure 6).[20]

The neutral molecule dithiolane exhibits according to a structure determination for the coenzyme α-lipoic acid $S_2(CH_2)_2CH(CH_2)_4COOH$ a dihedral angle ω(CS-SC) = 35°, which is caused by sulfur lone pair repulsion n_S/n_S.[20] For a comparison with the less electron-rich $SS^{\bullet\oplus}$ linkage in the radical cation, a pseudorational CNDO total energy hypersurface has been calculated for the $\Delta\varphi/\Delta\omega$-combined ring motion in the neutral molecule (Figure 6). Much to our surprise, the CNDO barrier for a H_2C swing from $\varphi = +50°$ to -50° overlaid by a twisting $\Delta\omega = \pm 30°$ amounts to only ≈ 10 kJ mol^{-1}. The CNDO hypersurface clearly indicates that the molecular rigidity increases with $H_2C(CH_2S)_2$ bending $\Delta\varphi$ and that the twisting motion $\Delta\omega$ becomes more important at values $\varphi > 20°$.

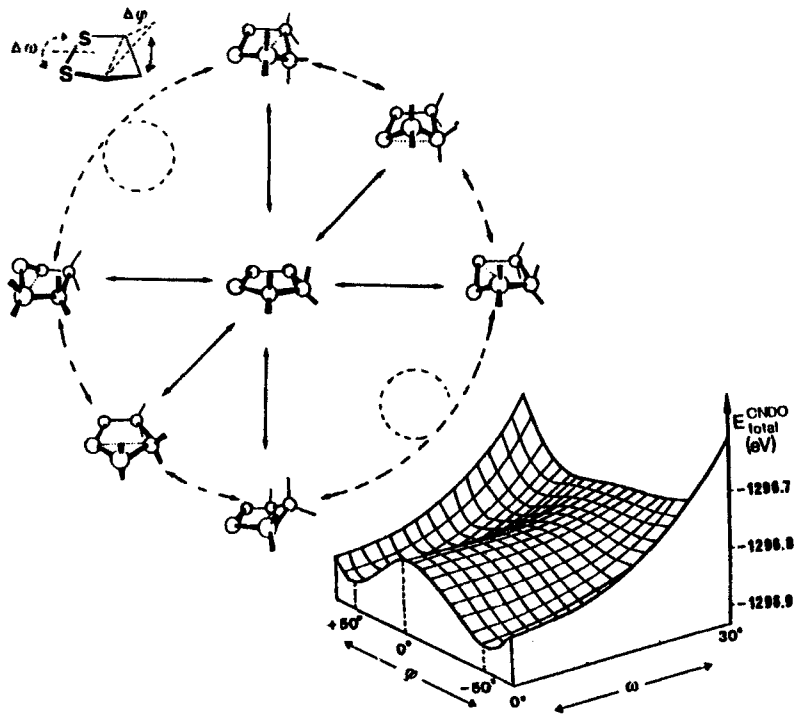

FIGURE 6 Pseudorotation motion of the dithiolane ring and CNDO total energy hypersurface for the combined $\Delta\varphi/\Delta\omega$ dynamics yielding a barrier of only $\approx$ 10 kJ mol^{-1} (cf. text).

The ring pseudorotation in dithiolane, therefore, should not be dominated by n_S/n_S repulsion and the $S_2(CH_2)_2CHR$ dihedral angle ω(CS-SC) $\approx 35^0$ determined for crystals of α-lipoic acid might well be partly due to a lattice packing effect.

Take Home Lesson: Molecular dynamics, which is of utmost importance for numerous reactions of molecules as an energy storage possibility, are accessible both experimentally as well as quantum-chemically for most cases with dominant population of specific ones out of the 3N-6 degrees of freedom. Relative to the "electron arrows" of organic reaction notation (Figure 2: A), the inclusion of molecular dynamics into the structure $\leftrightarrow$ energy relationship of the state model (Figure 2: B), although often rather difficult, is one of its tremendous advantages.

In order to emphasize the importance of molecular dynamics, as an additional example the CNDO total energy surface for SH rotation in thiophenol, made up of 17 x 35 = 595 individual CNDO calculations, is presented: [2]

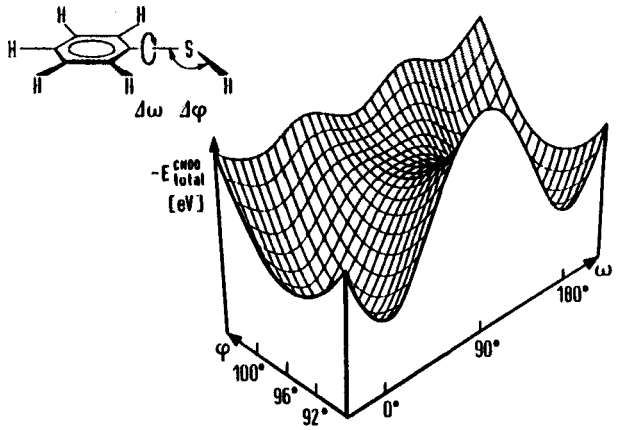

(10)

In addition to twisting Δω about the CS axis, deflections Δφ of the bending angle C-S-H also have to be considered, especially on passing of the ortho hydrogens of the benzene ring. Obviously no minima of the CNDO total energy occur except for planar arrangements at $\omega = 0^0$ and 180^0.

F. Microscopic Reaction Pathways: Approximate Energy-Hypersurfaces for Isomerization XSSX → X_2SS

Despite of most impressing femtosecond laser investigations of reaction pathways and transition states of small molecules in adiabatically cooled jet streams,[22] the preparative chemist is rather interested in medium-sized molecules with an usually prohibitive 3N-6 degrees of freedom. Nevertheless, information based on sequences of structure "snapshots" as searched from the Cambridge Structure Database,[23] can already provoke imagination and, above all, prevents "electron arrow" interpretations (Figure 2: A). Often, quantum chemical hypersurface elaborations for larger molecules, although necessarily incomplete and rather qualitative, are of help.[8,9,12]

One of the many prerequisites of such calculations is that either experimental information about the detailed reaction course is available or plausible assumptions are possible, as for the presumably intramolecular isomerization FS= SF → F_2S=S to the thermodynamically more stable of

the two.[24] For both isomers FSSF and F_2SS, which can be prepared separately, the experimental data such as ionization energies or dipole moments are satisfactorily reproduced by CNDO calculations.[24] Based on both the known gasphase reaction as well as the tested semiempirical calculation procedure and assuming, in addition, an intramolecular 1,2-fluorine shift, the energy hypersurface for the isomerization FSSF ↔ F_2SS (Figure 7 : A) is approximated in the following way: One fluorine migrates along the SS axis x of the fixed FSS fragment through 12 sectional planes z each with 144 screening pionts. The surface made up of 1728 CNDO total energies - neglecting configuration interaction, but with completely optimized geometry in the region of the minima - exhibits clearly an energetically preferred potential valley for the isomerization with the shallow minimum at the saddle point corresponding to an almost planar three-membered ring due to an F position above the S-S bond (Figure 7 : A).

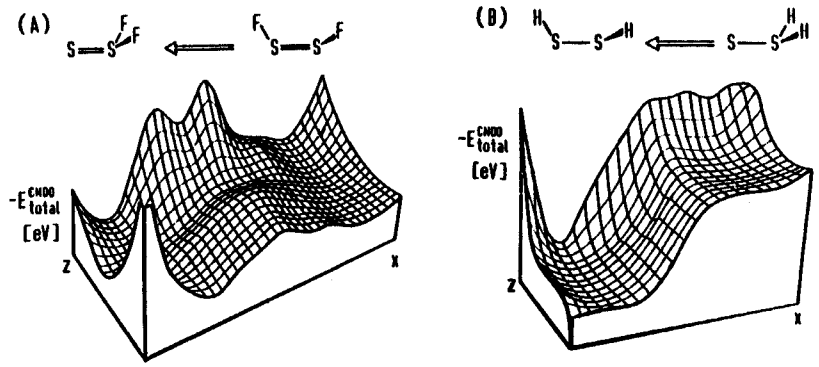

FIGURE 7 CNDO total energy hypersurface for valence isomerization XSSX ↔ X_2SS : (A) X = F and (B) X = H (see text).

The CNDO total energy hypersurface confirms F_2S = S to be the most stable isomer. For HSSH and also for ClSSCl, [24] however, any attempt to isolate the corresponding isomers Cl_2S=S or even H_2S=S (Figure 7: B) is predicted to be a futile effort: Both should be thermodynamically far less stable and, in addition, attributed to rather shallow minima with low barriers, they should also be kinetically unstable.

Take Home Lesson: With respect to the 3N-6 degrees of freedom in molecular dynamics (cf. chapter II. E), microscopic reaction pathways can

only be approximated by energy hypersurface calculations based on partly severe assumptions and simplifications. Despite of all the complexity, nevertheless, some conclusions are most valuable to the preparative chemist: For instance within the isomerization systems XSSX $\leftrightarrow$ X_2SS selected for illustration, the predictions in complete accord with experimental evidence are: Both isomers FSSF and F_2SS must be isolatable, F_2SS is the thermodynamically more stable one or the isomers H_2SS as well as Cl_2SS are both thermodynamically and kinetically unstable with respect to the isomers HSSH and ClSSCl.

Based on the qualitative molecular state model exemplified for selected sulfur compounds and including in addition to topology, symmetry, effective nuclear potentials, electron distribution and molecular dynamics even an approximate energy hypersurface pathway for the presumably intramolecular isomerization FS=SF $\rightarrow$ F_2S=S, three topics of sulfur research in Frankfurt will be discussed in more detail: the gasphase preparation of short-lived and partly interstellar molecules (chapter IV), the generation of radical ions in aprotic solutions (chapter I) and the crystal growth and structure determination of sulfur compounds (chapter V).

III. GASPHASE PREPARATION OF SHORT-LIVED SULFUR MOLECULES

A. Instrumentation, Gas Analysis and Optimization of Thermolysis Conditions

Radical cation state fingerprints of molecules recorded e.g. in photoelectron spectroscopic ionization patterns render possible an elegant real-time analysis of small amounts of compounds in flowing gas mixtures (Figure 3 and 4): [9-11] The thermolysis conditions can be optimized and the products including short-lived molecules identified. The instrumentation used depends largely on the problem and varies from short-parthway devices with partly electron-bombardment heated ovens for generation of kinetically unstable species under close to unimolecular conditions within a photoelectron spectrometer (11: A) to arrangements including several ovens [9,10] as well as cooling traps for the isolation of compounds thermally and/or catalytically prepared (11: B), which are on line-connected to a photoelectron spectrometer. [9-11]

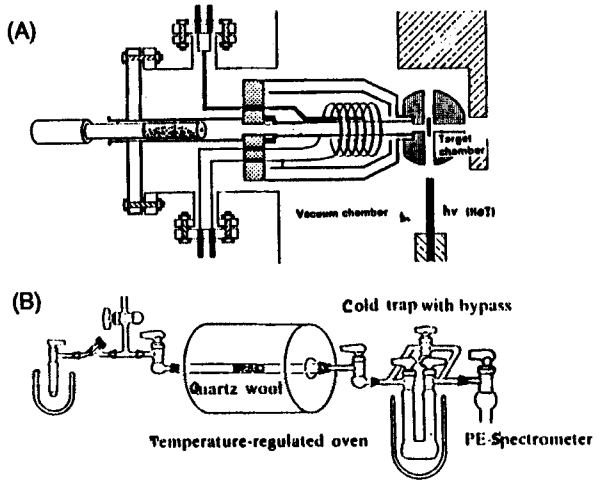

(11)

In the short-path pyrolysis apparatus integrated into a PE spectrometer (11: A), the distance between the end of the oven zone and the target chamber amounts to only 3 cm, which allows to record ionization patterns of molecules with half-live times down to about 10^{-4} seconds.[10,11] The building-block apparatus for investigations on a preparative scale (11: B) allows to isolate the thermolysis products in cold traps, to purify them by fractionate condensation and to characterize them in addition to their PE also by their MS or NMR spectra. [9-11] For the optimization of reaction conditions, which can be accomplished with less than a millimole of the compound within few hours, as well as in the identification of the products, the available possibility to add or to subtract digitally stored PE spectra on-line is of considerable advantage (Figure 7).

B. The Gasphase Preparation of Thiocarbonyl Compounds

For the exemplary case of thioacrolein, its generation by the thermolysis of diallylsulfide, the topological analysis of the product ensemble C_3H_4S, the identification of $H_2C{=}CH{-}HC{=}S$ and its isolation as Diels/Alder dimer has been presented (chapter II: A). The starting point of these investigations, however, had been the preparation of the interstellar molecule thioformaldehyd $H_2C{=}S$ - found e.g. in the Sagittarius nebula - on earth (Figure 7). [2, 8, 25, 26] By the thermolysis $H_3CSCl \rightarrow H_2C{=}S + HCl$ and consecutive removal of $HCl + NH_3 \rightarrow NH_4Cl$, the ionization pattern of pure $H_2C{=}S$ is recorded and unequivocally assigned by a (correlated) Greens-Function calculation of the radical cation state sequence.

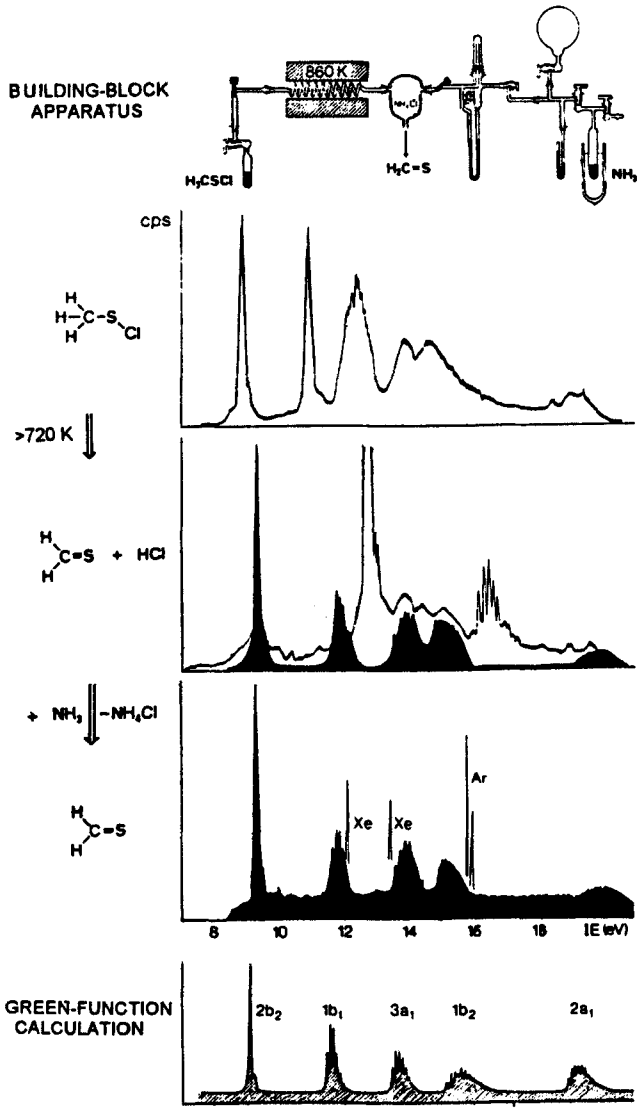

FIGURE 7 Preparation and identification of $H_2C{=}S$ in the gasphase: In the building block apparatus, H_3CSCl is decomposed above 720 K to a mixture of $H_2C{=}S$ + HCl, from which HCl is removed by stoichiometric NH_3 injection as solid NH_4Cl. The ionisation pattern of $H_2C{=}S$, calibrated with Xe and Ar, is assigned by spectra simulation based on a Green-Functions $M^{\bullet\oplus}$ state calculation (see text).

There are many more precursor molecules, which store their increasing thermal energy transferred predominantly from collisions of the heated reaction tube wall or its quartz wool filling in a way that they selectively fragment into a thermodynamically favorable "leaving molecule" and the target molecule $H_2C{=}S$: [25-28]

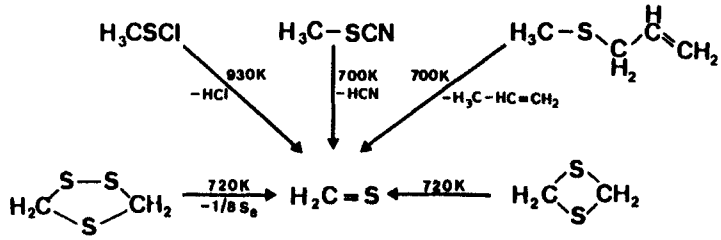

(12)

According to the decompositon temperatures (12), both propene and HCN eliminations are quite advantageous as is the sulfur extrusion from trithiolane $(CH_2)_2S_3$ or the monomerisation of dithietane ring dimers. These procedures prove to be valuable also for the thermal generation of other thioketones, which often can be isolated as trimers [28] or as for thioacrolein (3) as a mixture of Diels/Alder dimers:

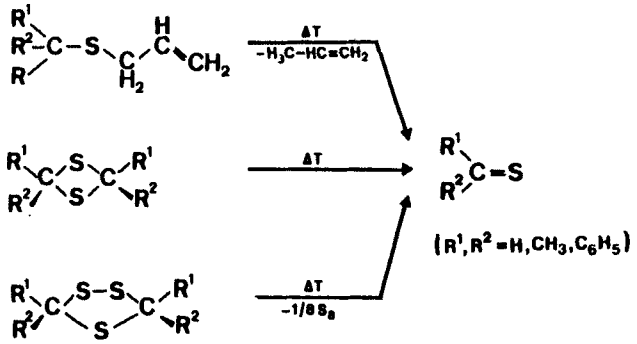

(13)

Trithiolane precursors are easily accessible from carbonyl compounds, H_2S and S_8. [26]

Along these lines, numerous thiocarbonyl derivatives have been prepared by usually highly selective thermolysis reactions in good yield: Thioketene is the only thermolysis product of both the N_2 elimination from 1,2,3-thiadiazole above 900 K - i.e. on passing through a red-glowing tube - and the H_2S abstraction from dithioacetic acid at about 170 K lower temperature (14: A). [30]

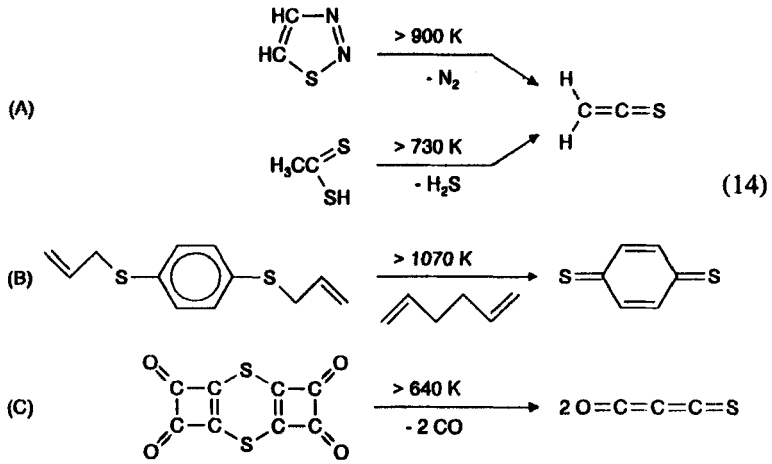

(14)

The preparation of matrix-trapped dithio-p-benzoquinone is accompanied by 1,5-hexadiene formation, presumably from two allyl radicals (14: B). [31] The third thiocarbonyl derivative presented, 3-thioxo-1,2-propadien-1-one, has been detected first in the interstellar nebula Taurus TMC 1 and is of interest to spectroscopists as a linear, but not pseudolinear molecule. It can be prepared in 100% yield and gram quantities under PE spectroscopically optimized thermolysis conditions (14: C) - another illustrative example on how chemists can profit by looking at molecular states (chapter I).

C. Unsaturated Sulfoxides X=S=O and Phosphorsulfides X-P(=S)$_{1,2}$

Presently many areas of inorganic chemistry are explored with tremendous speed and success - often even referred to as its "renaissance" - stretching from novel solid materials to the ocean of unsaturated main group element compounds discovered within the last two decades, partly by using PE spectroscopic gas analysis and comprising molecules such as phenyl sila-isonitrile H_5C_6-N≡Si with singly coordinated, triply bonded silicon. [9] From numerous rather unexpected sulfur molecules, two classes of compounds are selected here, unsaturated sulfoxides X=S=O (X = S; [33] H_2C [34] or HN [35]) and $\sigma^2\lambda^3$- or $\sigma^3\lambda^5$- thiophosphorus derivatives X-P=S (X = Cl [36] or F [37]) or X-P(=S)$_2$ (X = F, [37] Cl [38] or H_5C_2 [39]).

Sulfoxides: Sulfur burns in oxygen at low pressure to form a mixture of OSO and SSO. A steady gas stream of largely SSO can be generated by passing thionylchloride over solid silver oxide and its ionization pattern recorded via on-line connection to a PE spectrometer. [33]

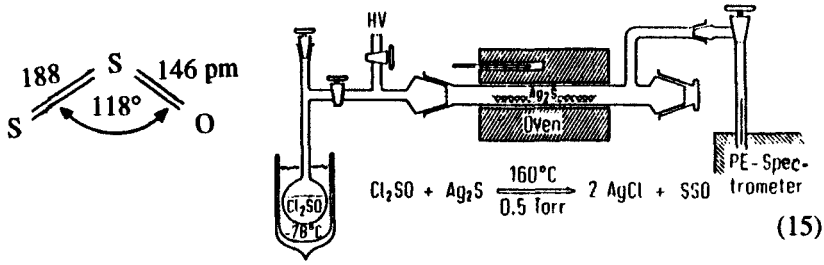

(15)

The state sequence of bent S=S=O$^{\bullet\oplus}$ assigned in orbital notation reads n_S^{end} (a') < Π_2(a") < n_S^{middle}(a') < Π_1(a") and the calculated charge distribution (-.23)–(+.73)–(-.50) is highly unsymmetrical.[33]

Another short-lived species defying all synthesis attempts has been sulfine $H_2C{=}S{=}O$, the S-oxide of thioformaldehyde (Figure 7). In the mean-time, it has been observed PE spectroscopically - partly together with $H_2C{=}S$ - in the a variety of flowing gases: [27,34]

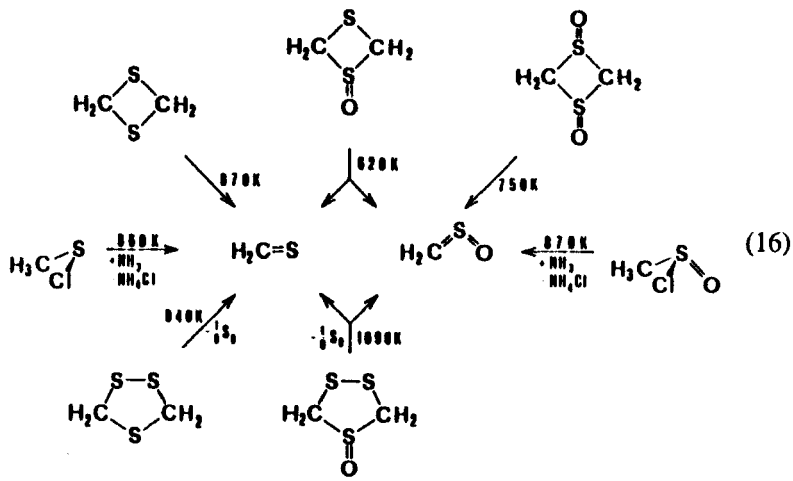

(16)

The third example concerns the nitrogen derivative HN=S=O, which is iso(valence)electronic to both the 16 electron molecules S=S=O (15) and $H_2C{=}S{=}O$ (16) and one of the transparent examples of a low-pressure gasphase synthesis, optimized by using PE spectroscopic molecular fingerprints: [11,35]

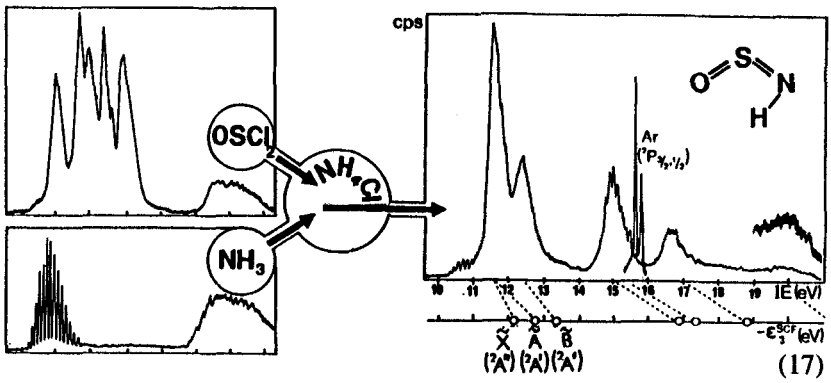

The ammonolysis of sulfinyl chloride occurs both spontaneously and quantitatively upon mixing the gaseous reactants in a reaction flask. The non-overlapping PE spectra of the three components of the flowing mixture allow one to quickly adjust the 3 : 1 stoichiometry, and to monitor it continuously. In the OSNH spectrum chosen here (17) and assigned via Koopmans' correlation with SCF eigenvalues, a small excess of NH_3 can be recognized by the low-intensity band between 10.5 to 11 eV exhibiting the well-known vibrational fine structure. [11,35]

$\sigma^2\lambda^3$- and $\sigma^3\lambda^5$-Thiophosphorus Derivates: The first compound prepared by passing phosphorus halides over heated silver wool had been O=P-Cl from $O{=}PCl_3$ above 1100 K, [36] because silver oxide decomposes already above 570 K. Although selectivity decreases for S=PCl from $S{=}PCl_3$ due to a second surface reaction channel to silver sulfide and PCl_3, still the "pure" SPCl PE spectrum can be obtained by digitally subtracting the PCl_3 ionization pattern from that of the resulting gas mixture (Figure 8). [36]

Other small molecules, which violate the outdated "non-double bond-rule" for main group elements of third or higher periods, are the σ^3/λ^5-thiophosphorus derivatives $X\text{-}P(=S)_2$. The prototype chloride is readily accessible from the corresponding pyridinium betaine (X = S): [38]

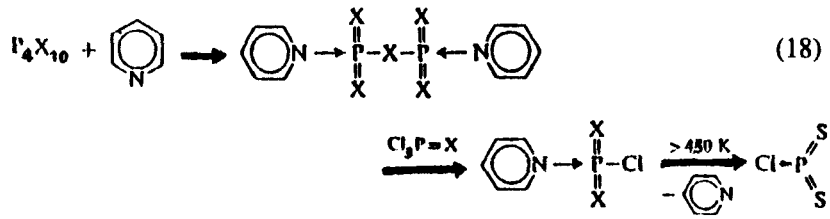

(18)

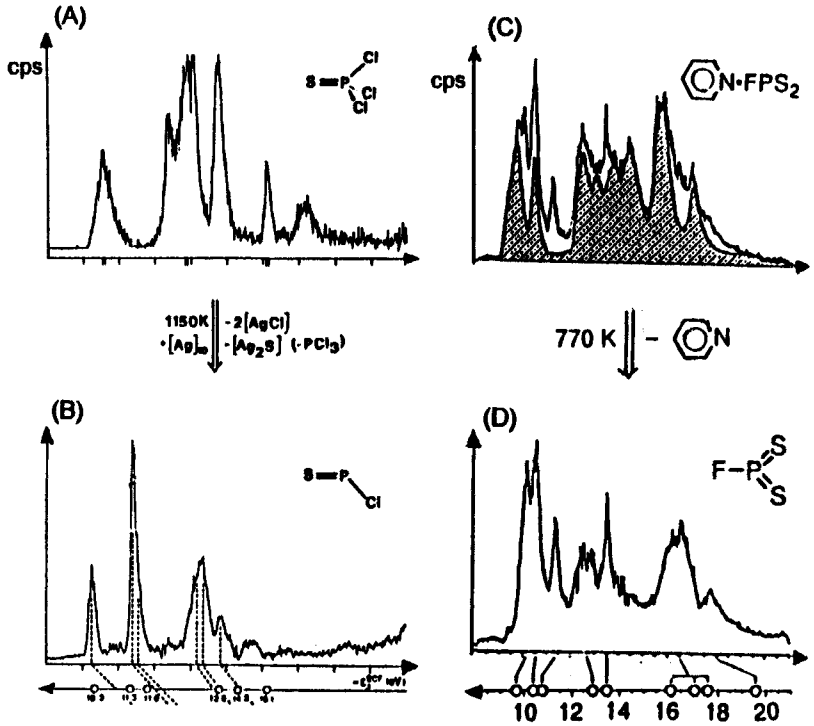

FIGURE 8 Gasphase preparation and PE-spectroscopic characterization of unsaturated thiophosphorus halides: (B) ClP=S after reaction of $SPCl_3$ (A) with silver wool at 1150 K and computer-subtraction of the ionization bands of the side product PCl_3 and (D) $FP(=S)_2$ recorded at 770 K after evaporation of $H_5C_5N{\cdot}FPS_2$ at 470 K (C) and after computer-subtraction of the pyridine PE spectrum (prerecorded, shaded). Both $M^{\bullet\oplus}$ state sequences are assigned by SCF eigenvalues via Koopmans' correlation $IE_n^v = -\varepsilon_j^{SCF}$. [36,37]

According to the continuously recorded PE spectra (Figure 8: C and D), evaporation under 10 Pa pressure leads to dissociation into the respective betaine components $X\text{-}P(=S)_2$ and pyridine. The ionization pattern of the $\sigma^3\lambda^5$-thiophosphorus derivatives such as $F\text{-}P(=S)_2$ (Figure 8: D) [37] can be "extracted" from that of the dissociation mixture by digital subtraction of a computer-stored pyridine PE spectrum (Figure 8: C, shaded). In addition other derivatives such as the reactive methyl and ethyl derivatives are easily synthesized by heating the preparatively accessible dimer precursors under reduced pressure ($R = CH_3, C_2H_5$): [39]

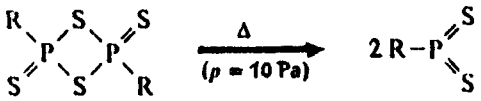

(19)

The molecules (18) and (19) extend the class of phosphorus(V) compounds Y-P(=X)$_2$ with three-coordinate phosphorus: The compounds generated in the gasphase are no longer stabilized kinetically by steric encapsulation. In addition, some of them are novel four-center molecules with 24 valence electrons and, therefore, allow most interesting molecular state comparison with analogous ones such as BCl_3, $Cl_2C{=}S$, Cl-NO_2 or SO_3. [38]

D. Energy Hypersurface Calculations for the Thermal S_2N_2 Monomerisation and Dipropargylsulfide Fragmentation

Referring to G. Pimentel's statement "Despite all that is known about reaction behaviour, understanding of it is rather shallow ...", our lack of knowledge about microscopic reaction pathways especially of medium-sized molecules has been reviewed repeatedly.[8] And despite intricate laser/ molecular beam experiments combined with numerically exact quantum chemical calculations shed more and more light on the reaction channels of atoms and/ or few-atom ensembles, in sharp contrast, it remains largely unknown so far, from which directions medium-sized molecules, energetically "hot" from preceding collisions, must collide to successfully penetrate each other and form the reaction complex, how their structures change during the energy transfer between them and what rôle molecular dynamics plays in this process.

Thermal S_2N_2 Monomerisation: Tetrasulfur tetranitride, S_4N_4, a cage with a square set of N centers and a bisphenoid of S centers, forms thermochromic crystals and must be handled with care, since friction, percussion , or rapid heating can cause it to explode. [40] When this compound is pumped through silver wool heated to 490 K, colorless crystals of square-planar S_2N_2, another literature-known explosive, can be isolated, which at room temperature polymerizes to the golden, lustrous, super-conducting $(SN)_x$. In the gasphase at low pressure, the sulfur nitrides $(SN)_4$, $(SN)_2$ and SN have been identified and characterized by their photoelectron spectra. [40] Based on our experience concerning the controlled thermal decomposition [5] of hazardous compounds like azides [1,5,6] in flow systems using PE spectroscopic real-time analysis, [5] we have

pyrolyzed S_4N_4 over silver wool at 10^{-2} mbar pressure and temperatures up to 1100 K. [40] The PE spectra recorded exhibit a marked temperature dependence: N_2 evolution starts already at about 800 K, and at 900 K all S_4N_4 is converted predominantly into S_2N_2. Comparison with known ionization patterns clearly demonstrates that two consecutive reaction channels are populated: one leading to the monomer SN and a second one unexpectedly producing SS, which is above 1100 K the preferred decomposition product. [40]

In order to rationalize qualitatively the PE spectroscopic observation that S_2N_2 decomposes preferentially into two SN molecules at lower temperatures, whereas SS and NN are favored at higher temperatures, an approximate MNDO hypersurface has been calculated based on the following assumptions: [40] S_2N_2 with six degrees of freedom can be approximated by starting from a tetrahedral arrangement and by projecting its deformation onto only two coordinates, the distance between SS and NN subunits as well as the dihedral angle ω between them. Despite of this rather crude approach, the resulting exploratory singlet MNDO hypersurface (Figure 9) satisfactorily reflects all PE spectroscopic observations: [40] For the assumed S_2N_2 tetrahedral arrangement, a rather shallow local minimum is calculated in contrast to the more pronounced ones for the two four-membered ring isomers. Without a discussion to what extent the semiempirical enthalpies ΔH_f^{MNDO} reflect thermal stabilities, these two isomers possibly can transform into each other by a "wagging" vibration crossing the tetrahedral arrangement (Figure 9: left-hand side).The SN alternating isomer, which according to the definition of the $d_{SS/NN}$ distance coordinate is located outside the hypersurface cut presented here and, presumably slightly distorted from planarity, should dissociate preferentially into two SN molecules. Another SN pathway could include the SNNS species with an elongated S···S bond, for which a shallow minimum is predicted on the $d_{SS/NN}/\omega$ hypersurface (Figure 9: lower left) and which on NN bond cleavage also would yield SN molecules as observed by PE spectroscopy at lower temperatures. [40] The other four-membered ring isomer of C_2 symmetry with SS and NN subunits (Figure 9: right-hand side) would be a likely precursor for fragmentation into SS + NN, which are predicted to be thermodynamically more stable than two SN molecules. The approximate two-dimensional hypersurface cut for the S_2N_2 ensemble (Figure 9), which allows to rationalize most of the experimental observations, therefore, invites a more rigorous theoretical treatment.

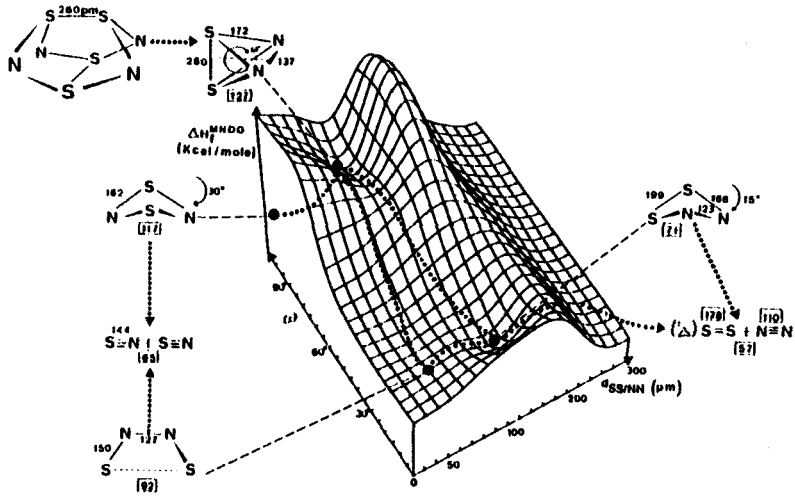

FIGURE 9 Exploratory singlet MNDO hypersurface for the deformation of the ensemble S_2N_2, projected onto the distance between SS and NN subunits in a tetrahedral arrangement as well as onto the dihedral angle ω defined with respect to this axis. For the individual species, which are partly located outside the truncated cut through the six-dimensional hyperspace shown here, the MNDO-optimized structural data are included as well as the approximate ΔH_f^{MNDO} values (positive, in kcal/mol) obtained for their minima.

Thermal Dipropargylsulfide Fragmentation: Thioaldehydes abound in diverse areas of nature: thus the parent molecule thioformaldehyd, which now can be prepared on earth in many ways [26] (Scheme 12), was first detected in interstellar space. [25] In contrast, its vinyl derivative thioacrolein, advantageously generated in the gas-phase by propene split-off from diallylsulfide and storable as a dimer [13] (Schemes 2 and 3) is found in the biosphere e.g. as one of the odorous components of garlic. [14] Quantum chemical evaluation predicts thioacrolein to be the most stable isomer out of thirteen, which are feasible with normal-valence topology within the ensemble C_3H_4S (Figure 3). In contrast, an analogous enthalpy of formation estimate for the more unsaturated ensemble C_3H_2S suggests a different sequence:

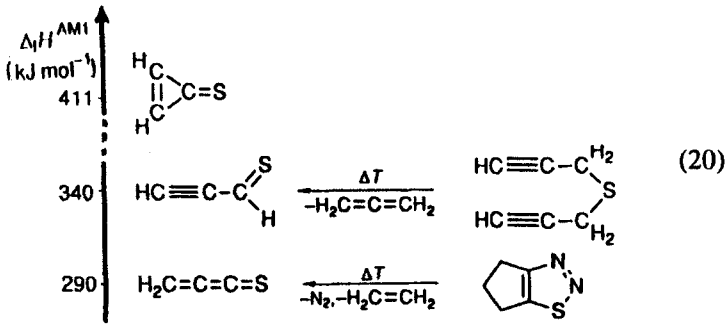

(20)

According to a literature survey, [41] the two valence isomers with the lower calculated enthalpies, propandienethione and propynethial, have been generated from different precursors (20), structurally characterized by microwave spectroscopy and isolated in a matrix. We have reinvestigated the thermal fragmentation of 2,2'-dipropynyl sulfide in a flow system at 10^{-3} mbar pressure between 300 to 1200 K by photoelectron spectroscopic gas analysis, [10, 11] and detected under the measurement conditions no traces of either the isomer $H_2C=C=C=S$, predicted to be thermodynamically more stable (20), or its anticipated degradation products HC≡CH and C=S. Therefore, and despite the twelve degrees of freedom for the six-center molecule HC≡CC(H)=S, the calculation of an approximate energy hypersurface for its gasphase generation under close to unimolecular conditions has been attempted (Figure 10).

Starting with the MNDO/CI optimized conformation of the precursor 2,2'-dipropynyl sulfide, a cis-configuration with a 60° dihedral angle between the two linear C-C≡CH subunits is predicted. The barrier to the saddle point should amount to about 220 kJmol^{-1} (Figure 10) and this value agrees well with the temperature of 830 K, at which the propynethial ionization peaks are first recognized in the PE spectra recorded continously of the heated flow system. The MNDO/CI optimized saddle-point geometry contains one bent $(H_2)CC=C(H)$ linkage, which allows the formation of a planar six-membered ring transition state with a rather short contact distance (H)C-H···C(H) of only 130 pm (Figure 10: ◕) and, consecutively, of the exclusive final products $H_2C=C=CH_2$ and HC≡C-HC=S. The enthalpy difference for the endothermic reaction is - despite of all the simplifying assumptions - estimated very reasonably to about 100 kJmol^{-1} (Figure 10). In addition, the MNDO/CI enthalpy hypersurface provides a rationale for the experimental fact that neither the precalculated more stable isomer $H_2C=C=C=S$ (20) nor its degradation

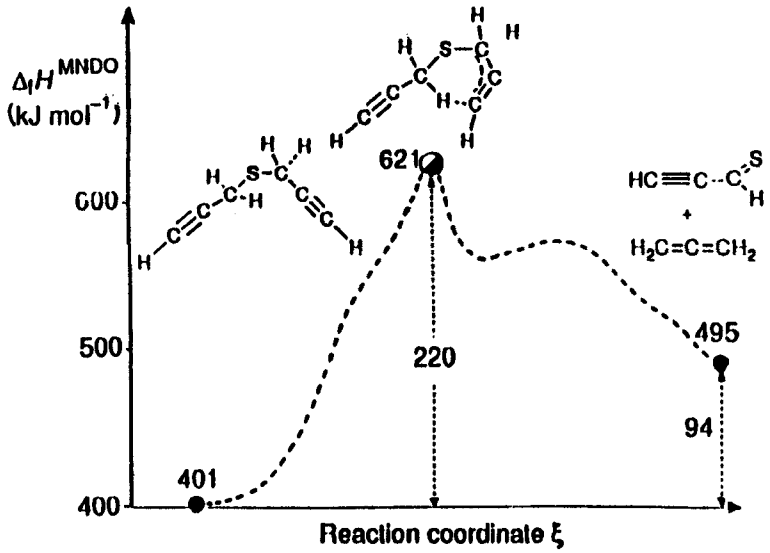

FIGURE 10 MNDO/CI enthalpy of formation hypersurface profile for an intramolecular thermal fragmentation of 2,2'-dipropynyl sulfide to propynethial and allene, based on the assumption that the coordinates chosen, $\Delta d_{C\text{-}H\cdots(C)}$ and $\Delta d_{S\text{-}C}$, represent the essential molecular dynamics. Along the presumable reaction pathway crossing the saddle point ◕ all structures have been MNDO/CI optimized. [41] (See text).

products could be detected photoelectron spectroscopically:[41] Its formation would require two hydrogens of the same H_2C group to move simultaneously and, therefore, the thermal fragmentation to the thermodynamically more stable isomer is kinetically forbidden.

In summary, the generation and identification of short-lived and mostly novel molecules can be advantageously studied by real-time photoelectron spectroscopic gas analysis. This approach not only allows to optimize reaction conditions for their preparation, but in addition to study the still largely unknown microscopic reaction pathways of medium-sized molecules with numerous degrees of freedom. Accompanying quantum chemical calculations help to rationalize the respective molecular states and their properties - much to the benefit of the preparative chemist.

IV. SULFUR-CONTAINING RADICAL IONS IN SOLUTION

In the introduction (chapter I) it has been pointed out that photoelectron spectroscopically determined ionization energies can be correlated via Koopmans' theorem, $IE_n^V = -\varepsilon_J^{SCF}$, to SCF eigenvalues and that ESR/ ENDOR signal patterns are supplementary (Figure 1):[2] The coupling constants, measured e.g. for π-type radical ions and proportional to π spin populations ρ_μ^π correspond according to the McConnell relationship, $a_X = |Q_X|\rho_\mu^\pi \propto |Q_X|(c_{J\mu}^\pi)^2$, to the "squared" coefficients of the respective, singly occupied molecular π orbital, $\Psi_J^{LCAO} = \Sigma\, c_{J\mu}\phi_\mu$. [2] In the following radical ion state report, therefore, first effects of thioalkyl substituents on π systems [2,42-44] will be characterized by data from both "eigenvalue" and "squared eigenfunction" spectrometers (chapter III: A). And a discussion of adiabatic ($t < 10^{-11}$ seconds) structural changes on single-electron redox reactions [5,45,46] (B) will precede an overview on reactions of organosulfur radical cations (C), [47-49] which are effective catalysts in the industrial 1,4-dichlorination of benzene. [50]

A. Alkylthio Substituent Effects

In classes of compunds with a common "parent" system of defined topology, potential changes by substituents within certain limits are profitably rationalized in terms of first and second order perturbations. [2-5] If, for instance, the benzene ring would be substituted in 1,4-positions with two XCH_3 groups, whose electron pairs n_X extend the π system, the changes in the π molecular state properties such as the ionization pattern (Figure 5 and chapter III: C) are usually satisfactorily approximated by 2nd order perturbation models:[2] The mixing of the symmetry-equivalent orbitals can be parametrized with PE ionization energies, based on those of unique symmetry representations serving as internal standards α_S and α_π. For the 1,4-bis(thiomethyl)- or -(methoxy)-substituted benzene derivatives selected as transparent examples (Figure 11), [2,42] it should be pointed out before any further discussion, that the numerical agreement of the lowest benzene π-ionization and the third ionization energy of the dithio compound (Figure 11: $\alpha_\pi = 9.25$ eV) guarantees the applicability of a 2nd order perturbation model.

Parametrisation of the $\pi_{C\text{-}S}$ and $\pi_{C\text{-}O}$ interactions by inserting the PE spectroscopic ionization energies results in values $\beta_{\pi S} = -1.1$ eV $< \beta_{\pi O} = -1.8$ eV: Due to more effective overlap, the $2p_C/2p_O$-perturbation exceeds the $2p_C/3p_S$ one considerably as already is evident from the 3.9 eV vs.

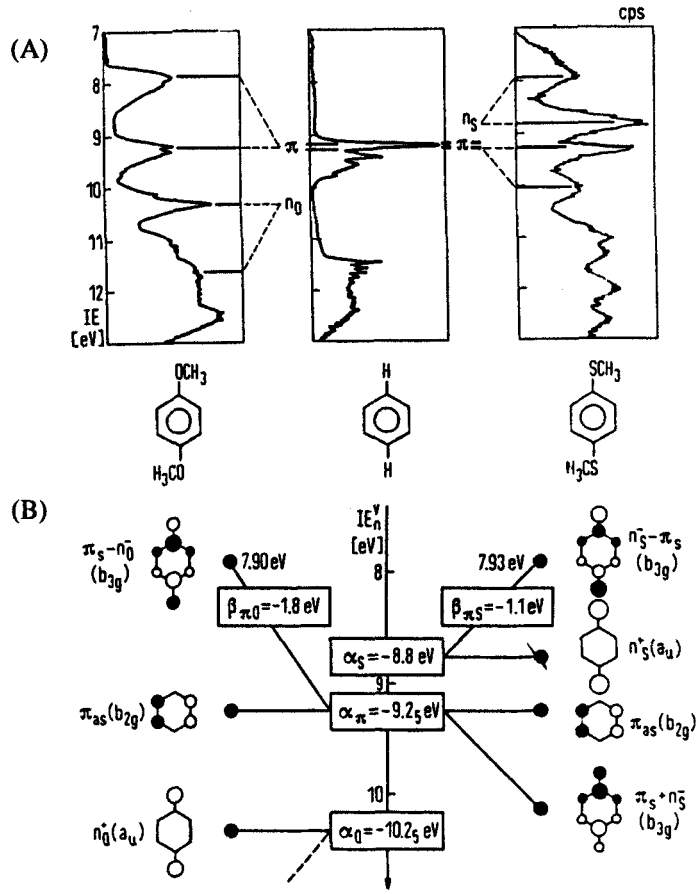

FIGURE 11 (A) The photoelectron spectra of benzene and its p-bis(methylthio)- and p-dimethoxy derivatives, which contain in their low energy region between 8 and 12 eV two or four ionizations to π radical cation states. (B) Second order perturbation MO model, in which the states of unique irreducible representation such as $n_S^+(a_u) \equiv \alpha_S$ and $\pi_{as}(b_{2g}) \equiv \alpha_\pi$ of the dithio π system represent internal standards and in which mixing of symmetry-equivalent orbitals $n_S^- \pm \pi_s(b_{3g})$ leads to mirror image splitting $\pm\delta\varepsilon_\pi$. The interaction parameters β, obtained as second order determinant solutions, $\beta\pi x = -\sqrt{(IE_2 - IE_1)(IE_3 - IE_1)}$, with vertical ionization energies as eigenvalues, clearly demonstrate that $2p_C/2p_O$ interactions are larger than $2p_C/3p_S$ second order pertubation. (See text).

2.1 eV splits n_O/π vs. n_S/π in the photoelectron spectra of 1,4-bis(methoxy)- and 1,4-bis(methylthio)benzenes (Figure 11: A).

Referring to numerous known examples,[2-5] a once established second order perturbation model will also reflect all other correlatable molecular properties such as the measured ESR spin populations of the corresponding radical cation: [2,42]

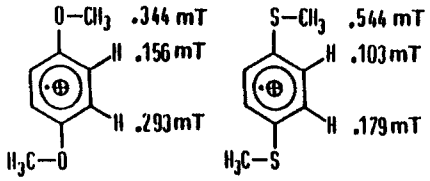

(21)

According to different mixing $n_X \pm \pi_S$ of the symmetry-equivalent b_{3g} components (Figure 11: B), a large ring π_S contribution is expected and observed for the dimethoxy derivative, in contrast to a large electron pair n_S contribution for the bis(methylthio)-substituted benzene radical cation, which shows in the relatively large H_3C couplings. [2,45]

Accordingly, thioalkyl groups are strong electron donor substituents in the ground state of radical cations as is demonstrated also for the corresponding 1,4-disubstituted naphthalene derivative by both the large g value increased due to S spin/orbit contribution and the again (21) relatively large H_3C hydrogen coupling: [43]

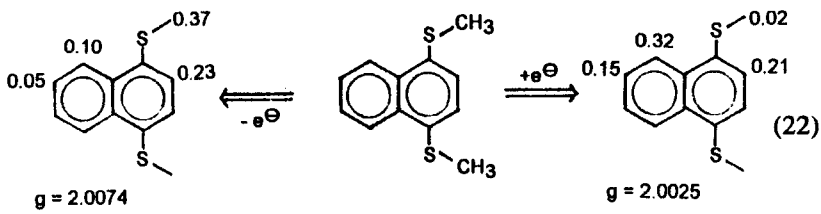

(22)

The radical anion, on the contrary, is characterized by each a low g value and H_3C hydrogen coupling, but rather large ring hydrogen coupling constants: Due to the thioalkyl donor substituents most of the spin and charge are distributed over the naphthalene ring. [43]

In addition to substituent effects, radical ions including those of sulfur compounds can be stabilized by other interactions such as contact ion pair formation [5] or, according to the molecular state model (Figure 2: B) by structural deformation: In the ENDOR spectrum of tetra(thioisopropyl)-p-benzosemiquinone radical anion, generated in THF solution by potassium

mirror reduction in the presence of lithium tetraphenylborate, the $^{7}Li^{\oplus}$ coupling is clearly visible: [44]

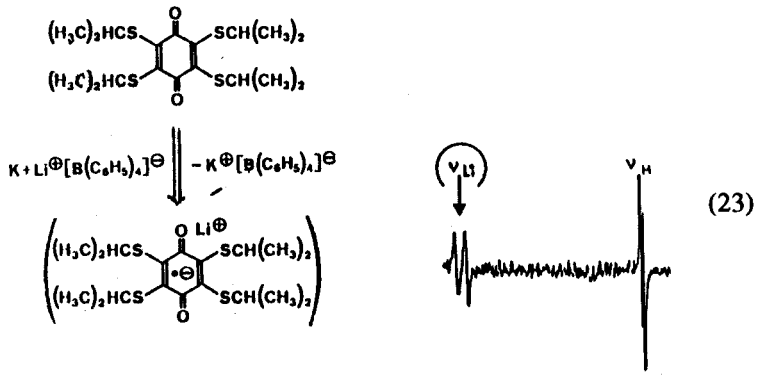

(23)

For a stabilizing structural deformation, the example of dithiolane radical cation $^{\bullet\oplus}S_2(CH_3)_2$ (chapter II: E) will be selected: on single electron oxidation, the dihedral angle ω (CS-SC) = 35° of the neutral molecule [20] should decrease to 0° due to optimum charge delocalization. This result of a geometry-optimized radical cation calculation agrees with all experimental observations such as the dynamics (9) or the oxidation potential. The generation in H_2CCl_2 solution has been accomplished by the powerful, water and oxygen-free and aprotic, selective one-electron oxidation system $AlCl_3$/ H_2CCl_2: [45]

$$H_2CCl_2 \xrightarrow[-[AlCl_4^{\ominus}]]{AlCl_3} (H_2CCl^{\oplus}) \xrightarrow[M^{\bullet\oplus}]{M} (H_2CCl^{\bullet}) \rightsquigarrow ClH_2C\text{-}CH_2Cl \qquad (24)$$

Its oxitation potential of ~ + 1.7 V corresponds to a first vertical ionization energy of ~ 8.0 eV. Therefore, dithiolane with IE_1^{V} = 8.25 eV needs an additional stabilizing distortion to the planar radical cation to be oxidized at all by $AlCl_3$/ H_2CCl_2, the one-electron oxidation system especially recommended for organosulfur compounds. [21, 43,45-52]

B. Structural Changes on Single-Electron Oxidation of Sulfur Compounds

Electron-rich molecules i.e. those with nonbonding electron pairs such as organic sulfides are especially susceptible to structural changes even on one-electron oxidation. [2,5] The skeletal distortion can be predicted and/ or

rationalized by quantum chemical total energy hypersurfaces as illustrated for the radical cation of bis(dimethylamino)disulfide after CPU-time saving exchange $H_3C \rightarrow H$ (Figure 12). [5,46]

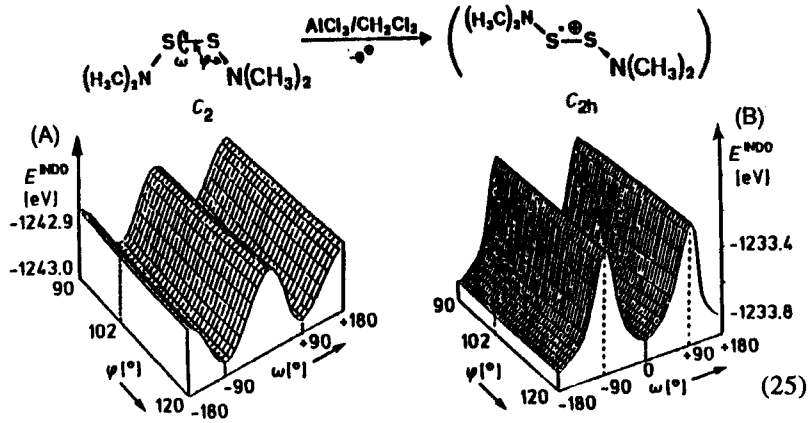

(25)

The INDO total energy surfaces for the model compound H_2NSSNH_2 are based on the dihedral angle ω(NS-SN) and the obtuse angle φ(SSN), which have been selected as coordinates out of its 3N-6 = 18 degrees of freedom. Their comparison (25) not only allows to rationalize the single-electron oxidation of the experimentally studied bis(dimethylamino)-disulfide, but also illustrates the time-dependence of the radical cation generation by vertical ionization (25: A) and by adiabatically relaxed oxidation (25: B).

The vertical ionization of $(H_3C_2)N\text{-}SS\text{-}N(CH_3)_2$ at 8.02 eV generates its radical cation ground state of unchanged C_2 symmetry (Figure 12: A) within about 10^{-15} seconds and with the positive charge largely delocalized over the N and S centered lone pairs. The first adiabatic ionization energy is observed about 0.8 eV = 77 kJ mol^{-1} lower at 7.2 eV and due to the vibrational relaxation below 10^{-12} seconds with a changed structure. The ESR spectrum registered with a time resolution of greater than 10^{-8} seconds after one-electron oxidation with $AlCl_3$ in H_2CCl_2 (24) proves planarization to a radical cation of C_{2h} symmetry. Further confirmation is provided by the INDO closed- and open-shell energy hypersurface calculations for the model compound $H_2N\text{-}SS\text{-}NH_2$, (25) which predict a dihedral angle ω(NS-SN) of 90° for the neutral compound and, in accord with the registered ESR signal pattern in solution, 0° for its planarized radical cation. [46]

Frequently, adiabatic structural changes observed on one-electron oxidation of organosulfur compounds exceed those within conformational dynamics. For example, treatment of sulfurnitride derivatives with $AlCl_3$ in H_2CCl_2 (24) usually produces - after the delay-time noted in (26) - the ESR signal pattern of the obvioulv thermodynamically favorable and structurally characterized radical cation $^{\bullet\oplus}S_3N_2$: [47]

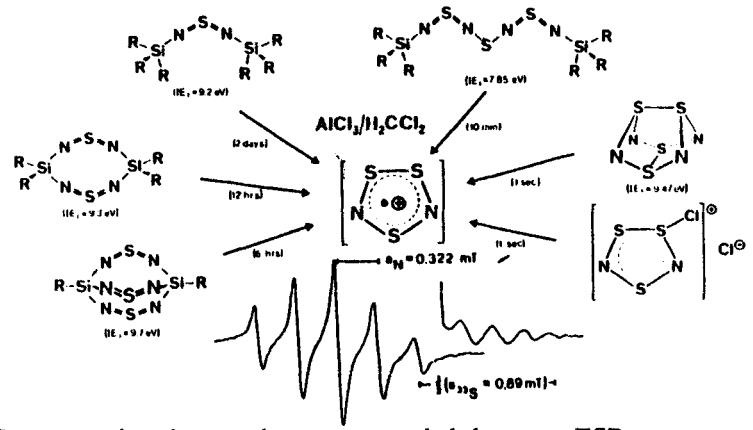

(26)

Some caution has to be recommended because ESR spectra can be recorded in concentrations below 10^{-5} mol and, therefore, the paramagnetic $^{\bullet\oplus}S_3N_2$ might only be produced in trace quantities. On the other hand, tremendous structural changes are observed also on oxidation of other organic sulfides such as the sterically overcrowded hexakis(thioalkyl)ethane: [48]

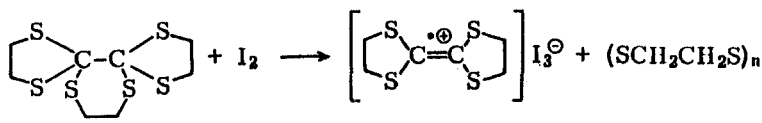

(27)

The one-electron oxidation can also be accomplished by $AlCl_3$ or $NO^{\oplus}$ $BF_4^{\ominus}$ and is easily recognizable due to the violet colour of tetrahydrotetrathiofulvalene radical cation. [48]

C. Reactions of Sulfur Radical Cations

The advantageous generation of organosulfur radical cations by using the superb $AlCl_3/H_2CCl_2$ single-electron oxidation system (24) [45] as well as their detection and characterization by applying the sensitive and highly resolved ENDOR line pair signal technique, [21] allows an easy access to study their numerous reactions.

Other termodynamically favorable organosulfur radical cations which form under widely varied reaction conditions, are the ones of dithiete [47, 49-51] (28: A) and benzodithiete derivatives (28: B) [51, 52]:

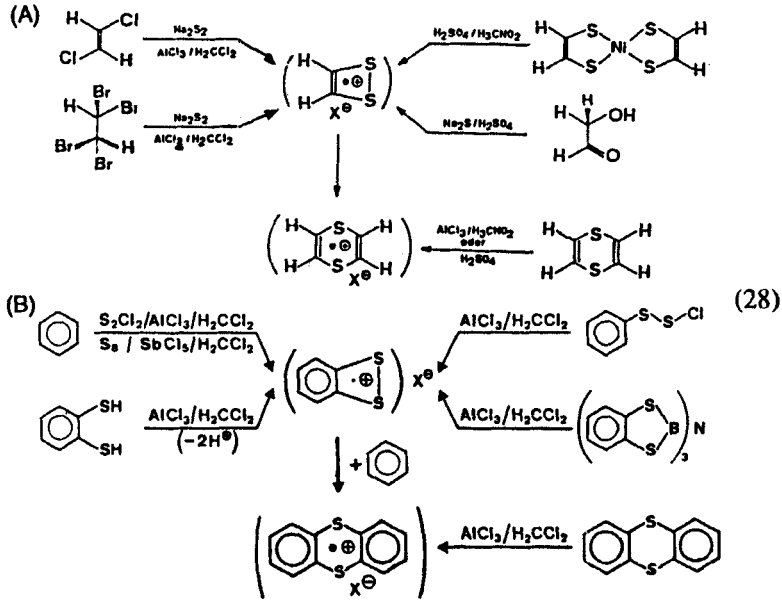

(28)

To the overall reaction scheme (28: A) from only partly sulfur-containing precursors, the Frankfurt group has added all the one-electron oxidations with $AlCl_3/H_2CCl_2$ [46, 49-51] as well as some prototype generations of dithiete radical cations from acetylene precursors and S_2Cl_2 (29) [50, 51]:

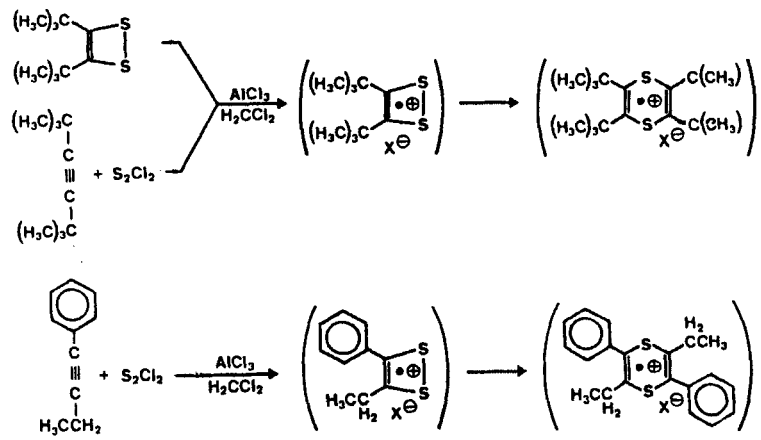

(29)

The unequivocal assignment of both the ESR/ENDOR signal patterns to final products such hexadithiane (28: A and 29) or thianthrene (28: B) radical cations took us by surprise, although again the 10^{-6} molar solution ESR detection limit has to be pointed out.

The ESR investigations on formation and reactions of dithiete radical cations (28 and 29) suggest a pathway for the catalysis of a preferred 1,4-dichlorination of benzene, carried out under Friedl/Crafts conditions on industrial scale with either elemental sulfur or organosulfur compounds: [52]

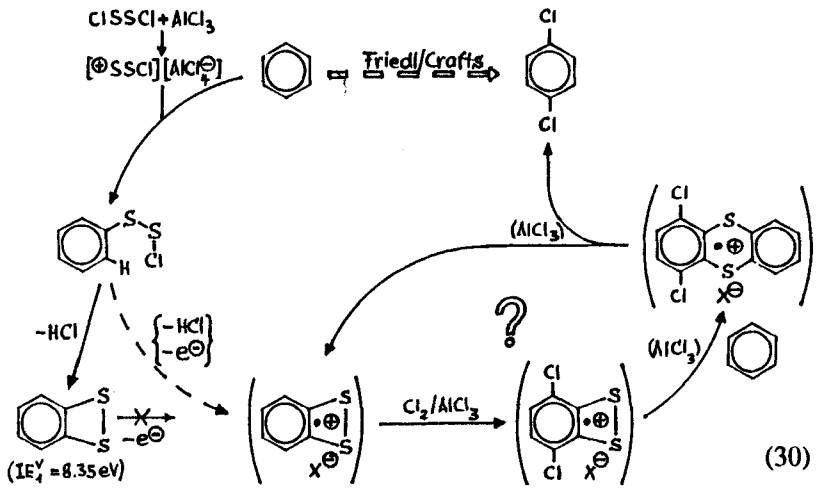

(30)

According to SCF calculations, the highest π electron densities are predicted at 1,4 ring centers of benzodithiete radical cation, which accordingly should be preferentially chlorinated by electrophilic attack. Thianthrene and eventually benzodithiete radical cation formation could possibly close the catalytic cycle to 1,4-dichlorobenzene. [52] If so, then again molecular state-directed (Figure 2: B) spectroscopic investigations would have provided valuable information.

V. WEAK INTERACTIONS IN MOLECULAR CRYSTALS OF ORGANOSULFUR COMPOUNDS

Molecular crystals contain organosulfur compounds in their respective ground state close to or even in their global energy minima and with largely "frozen" molecular dynamics. An analysis of crystal structures, therefore, serves as an advantageous starting point for the discussion of

numerous molecular properties and their quantum chemical calculation. [5] An additional crystal lattice analysis provides information on weak intermolecular interactions and, thereby, some static aspects of molecular self-organization. [67]

Referring to the structural changes already discussed for the butterfly-shaped 2,3,5,6-tetramethoxy-thianthrene, its planar radical cation and its cyanine distorted dication (7), three additional facets of molecular crystals as revealed by their structure determination will be presented. Examples are given each for a reaction intermediate, for weak interactions of for self-organization in crystals. They report on the 5-membered ring-opening on sodium reduction of dibenzothiophene, [53] the donor/acceptor interactions in the "charge transfer" complex {1,2,4,5-tetra-(isopropylthio)benzene···Br-Br}[54] and the tremendous lattice differences between orthorhombic and monoclinic polymorphs of 2,3,5,6-tetramethoxythianthrene. [55]

Thiophene Ring Opening on Sodium Reduction: Metal mirror reaction under aprotic conditions ($c_H\oplus$ < 0.1 ppm) often allow to isolate otherwise inaccessible compounds as crystalline residues, which immediately ignite on contact with air. In the example selected, dibenzothiophene opens on sodium metal reduction the five-membered unsaturated sulfur ring to form a diglyme solvated dimer salt (diglyme $Na^{\oplus}{}^{\ominus}S\text{-}C_6H_4\text{-}C_6H_5)_2$: [53]

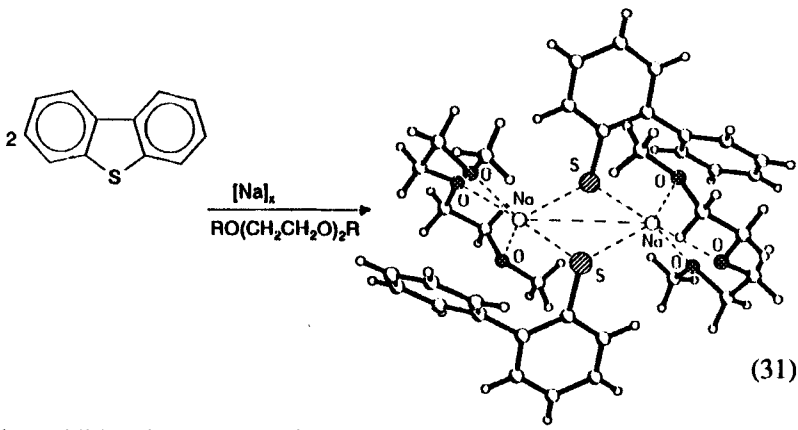

(31)

The additional hydrogen for the second phenyl ring is presumably provided by H abstraction from the ether. [5] Intriguing is the potential driving force of the ring-opening reaction: the $Na^{\oplus}$ cations of the four-membered ionic core $(Na^{\oplus}{}^{\ominus}S\text{-})_2$ are optimally solvated by the threefold O-coordinating polyether ether diglyme.[56]

Recognizable Electron Transfer in an Organosulfur Charge Transfer Complex: Single crystal growth of π complexes, in which donor and acceptor components are not stacked in different staples but rather interact with each other in stoichiometric ratios, can be successfully designed based on the criteria of identical skeletal symmetry and an approximately comparable overlap area. However, structures determined for e.g. {Tetramethoxy-thianthrene···Tetracyanobenzene} or {Thianthrene··· Pyromellitic Acid} do not show significant structural changes: Not even the interplanar angle of the thianthrene donors, the least energy demanding distortion, deviates from that in the respective neutral molecules. Therefore, presently smaller donor or acceptor molecules are investigated. [54]

Cooling of a tetrachloromethane solution containing 1,2,3,5-tetra(thioethyl)benzene and bromine in 1:2 ratio produces black blocks, which surprisingly consist of tetrathiobenzene layers interconnected alternatingly by bromine sticks:[54]

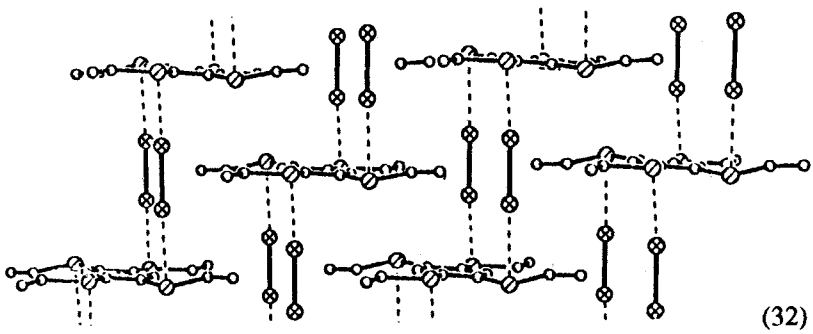

(32)

Relative to Br_2 molecules in the gasphase, the distance Br-Br is elongated from 227 to 240 pm, substantiating the charge transfer S → Br from the sulfur donor centers.

Orthorhombic and Monoclinic Modifications of 2,3,5,6-Tetramethoxythianthrene: Molecules with N centers and, accordingly, 3N-6 degrees of freedom, frequently float across the energy hypersurface with numerous local minima, in which they can be isolated as crystals of polymorphic modifications with only small differences in lattice(sublimation)energies.[7,56,57] In addition to serendipitous discoveries, often crystal growths under skilfully chosen optimum conditions allow to capture certain molecular conformations or lattice arrangements as fascinating molecular dynamics snapshots.

An interesting organosulfur example is 2,3,7,8-tetramethoxy-thianthrene, which crystallizes from diisopropyl ether solution in a monoclinic and from n-hexane solution in an orthorhombic modification. [53] Their structural differences are rather small (Figure 13: top): Comparison reveals that only the methoxy group in 2-position is twisted by 79° out of the plane of the adjacent six-membered ring (Figure 12: A). Nevertheless, this small structure perturbation causes a tremendous change in the lattice arrangement relative to the monoclinic modification (Figure 12: B), which contains in its unit cell altogether Z = 12 molecules of three different geometries.

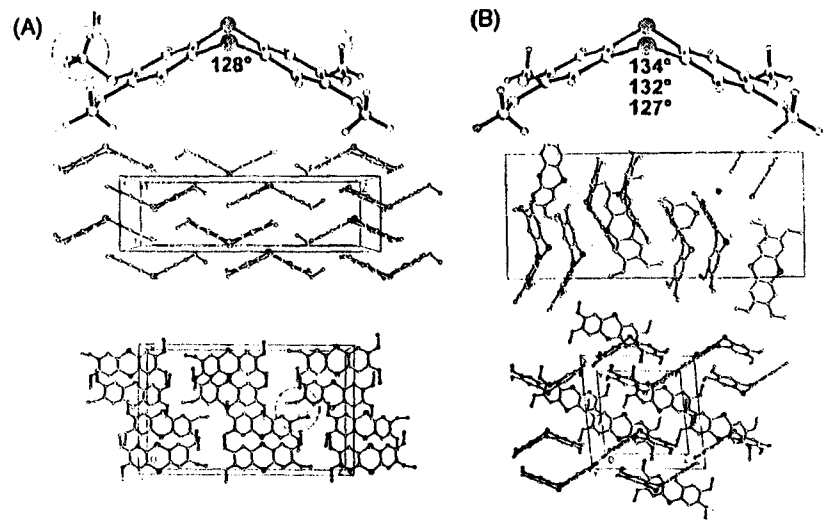

FIGURE 12 Polymorphic modifications of 2,3,7,8-tetramethoxy-thianthrene: (A) orthorhombic (Pbca, d(300 K) = 1.437 gcm^{-3}) with a dihedral angle of 128° and with its unit cell (Z = 8) in X and Y directions (circles: structure difference and lattice change) and (B) monoclinic ($P2_1/n$, d(300 K) = 1.395 gcm^{-3}) containing three independent molecules with different dihedral angles of 134°, 132° and 127° as well as unit cell (Z = 12) in X and Y directions. (See text).

The discussion of the orthorhombic and monoclinic modifications best starts from the structural point of view: Twisting of one H_3CO substituent not only reduces the sterical overlap between the methyl group and ortho hydrogens of the adjacent phenyl ring, but also allows a thermodynamically favorable, more dense lattice packing (Figure 12: A, shaded circles). Together these two effects overcompensate the lost n_O/π-interaction.

The crystal density difference at room temperature between the orthorhombic (1.437 gcm^{-3}) and the monoclinic (1.395 gcm^{-3}) lattice packing amounts to 2.6% and according to the lattice(sublimation)energies calculated by the atom/atom potential approximation, the orthorhombic modification of 2,3,7,8-tetramethoxythianthrene (-34.7 kJ mol^{-1}) is predicted to be more stable than its monoclinic one (-32.3 kJ mol^{-1}). For the crystal growth of the two different modifications, the following proposal is forwarded for discussion: The monoclinic crystal of lower density and lattice energy should grow from the solution in polar diisopropylether rather fast in a kinetically controlled way, whereas the orthorhombic one with higher density and lattice energy presumably grows thermodynamically controlled from the solution in an unpolar hydrocarbon.

Structural Information Recommendation: The three examples presented provide otherwise inaccessible information especially on intra- and intermolecular interactions in crystals, stretching from strong cation solvation to weak van der Waals forces. Therefore, the crystal growths of well-designed organosulfur compounds, even if demanding skill and tenacity, is strongly recommended.[5-7] And, as is pointed out also for discussions of structural information, the qualitative molecular state model emphasizing the rather important structure ↔ energy relationship (Figure 2: B) proves to be superior to the old-fashioned and outdated bonding concept (Figure 2: A).

VI. RETROSPECTIVE AND PERSPECTIVE: THE MOLECULAR STATES OF SULFUR COMPOUNDS

This lecture abstract summarizes for the first time our investigations on low-coordinate (organo)sulfur compounds and proposes as a rationale for their multifaceted properties a qualitative molecular state model, which in addition to the connectivity between centers, their three-dimensional arrangement, their potentials and the respective electron distribution, emphasizes structure ↔ energy relationships including molecular dynamics (Figure 2: B).

Faced with the "torrent" of novel organosulfur compounds and the "sea" of their molecular states, therefore, this report can illustrate at best only some aspects of selected examples investigated predominantly by

"eigenvalue" PE spectrocopy in the gas phase, "eigenfunction" ESR/ENDOR spectroscopy in solution as well as "weak interaction" structure determination in molecular crystals. The results confirm that suitable correlations of experimental and molecular-state data together with approximate quantum chemical energy hypersurface calculations do indeed allow a satisfactory rationalization of (organo)sulfur compounds and their numerous fascinating properties - including those of short-lived compounds. And the molecular state approach advertised has stood the test of applicability convincingly and, therefore, should be of considerable help also to the preparative chemist, who often likes to classify the multiplicity of his chemical species by chemical intuition and sometimes (already) by perturbation arguments, for instance, concerning substituent effects. Because these points of views do not differ much and as a complementary approach, the comparison of equivalent states of chemically related molecules based on their measurement data [2] is especially suggested for (organo)sulfur compounds.

Nevertheless, despite attempts of tentative interpretation, many questions pertinent to novel properties especially of larger molecules and their cooperative behaviour in aggregates and clusters remain unanswered - at least presently. Therefore, and by no means contradicting the impressing success of the qualitative molecular state approach presented, there may be more questions raised than answered in this report or, put positively, there is stimulation for numerous future experiments.

ACKNOWLEDGEMENT: The various research projects have been supported by the Deutsche Forschungsgemeinschaft, the State of Hesse, the Fonds der Chemischen Industrie and the A. Messer Foundation. In addition, gratefulness is expressed to all, who have helped us in our continuous learning process. And, above all, special thanks go to the dedicated coworkers, whose individual contributions are specified in the references cited.

REFERENCES

1. Essay 29 on Molecular Properties and Models. For essay 28 see H. Bock "Novel Hydrogen-bridged Molecular Aggregates: Design, Structures and Potential Calculations", Phosphorus, Sulfur, Silicon Rel. El. 87, 23 (1994).
2. H. Bock "Molecular States and Molecular Orbitals" Angew. Chem. 89, 631 (1977); Angew. Chem. Int. Ed. Engl. 16, 613 (1977) and lit. cit.
3. Cf. the review H. Bock "Molecular States of Silicon Containing Compounds" Angew. Chem. 101, 1659 (1989); Angew. Chem. Int. Ed. Engl. 28, 1627 (1989) and references therein.
4. Cf. the review H. Bock and W. Kaim "Organosilicon Radical Cations", Acc. Chem. Res. 15, 9 (1982).
5. Cf. the review H. Bock, K. Ruppert, C. Näther, Z. Havlas, H.-F. Herrmann, C. Arad, I. Göbel, A. John, J. Meuret, S. Nick, A. Rauschenbach, W. Seitz, T. Vaupel and B. Solouki, "Distorted Molecules: Perturbation Design, Preparation and Structures", Angew. Chem. 104, 564 (1992); Angew. Chem. Int. Ed. Engl. 31, 550 (1992) and references therein.
6. H. Bock, "Crystallization as a Model for Molecular Self-Organization?", Annals 1992 of the German Academy of Natural Scientists Leopoldina, 38, 221 (1993) and lit. cit.
7. H. Bock, "Some Static Aspects of Molecular Self-Organization from Single Crystal Structural Data", Mol. Cryst. Liqu. Cryst. 240, 155 (1994).
8. H. Bock, "How Do Medium-Sized Molecules Actually React?" Cf. the detailed reports on lectures at the Academy of Science and Literature in Mainz (Abh. Math.-Naturw. Klasse, 1986/2., F. Steiner Verlag, Wiesbaden), the Deutsche Akademie der Naturforscher Leopoldina in Halle (Nova Acta Leopoldina, Neue Folge 59, 93 (1985)), the 8. Journees Scientifiques, Deauville (L'actualite Chim. 3, 33 (1986)) or the 2. International Workshop, Königstein (Polyhedron 7, 2429 (1988)) and each references therein.
9. Cf. the review H. Bock and R. Dammel "The Pyrolysis of Azides in the Gasphase" Angew. Chem. 99, 503 (1987); Angew. Chem. Int. Ed. Engl. 26, 489 (1987).

10. For PE-spectroscopic gas analysis cf. the summary by H. Bock, B. Solouki, S. Aygen, M. Bankmann, O. Breuer, R. Dammel, J. Dörr, M. Haun, T. Hirabayashi, D. Jaculi, J. Mintzer, S. Mohmand, H. Müller, P. Rosmus, B. Roth, J. Wittmann and H.-P. Wolf, J. Mol. Structure 173, 31 (1988) and lit. cit., especially [11].
11. H. Bock and B. Solouki, Angew. Chem. 93, 425 (1981); Angew. Chem. Int. Ed. Engl. 20, 427 (1981).
12. For approximate calculations of energy hypersurfaces cf. the summary by H. Bock, R. Dammel and B. Roth in "Inorganic Rings and Clusters" (Hrsgb. A. Cowley), ACS Symposium Series, Vol. 232 (1983), p. 139 and lit. cit.
13. H. Bock, S. Mohmand, T. Hirabayashi and A. Semkow, Chem. Ber. 115, 1339 (1982) as well as J. Amer. Chem. Soc. 104, 312 (1982).
14. E. Block, Scientific American 252, 114 (1985).
15. H. Bock, W. Ried and U. Stein, Chem. 114, 673 (1981).
16. B. Beagley, V. Ulbrecht, S. Katsumata, D.R. Lloyd, J.A. Connor and G.A. Hudson, J. Chem. Soc. Faraday Trans. II 73, 1278 (1977).
17. A.D. Walsh, J. Chem. Soc. 1953, 2260; cf. also R. Buenker and S.D. Peyerimhoff, Chem. Rev. 74, 127 (1974) and references cited therein.
18. See, for example, E. Heilbronner and H. Bock: "Das HMO-Modell und seine Anwendung", Band I to III, Verlag Chemie, Weinheim 1968-1970; The HMO Model and Its Application, Wiley, New York 1975/1976. Japanese translation: Hirokawa, Tokyo 1973; Chinese translation: Kirin University Press 1983.
19. H. Bock, A. Rauschenbach, K. Ruppert and Z. Havlas, Angew. Chem. 103, 706 (1991); Angew. Chem. Int. Ed. Engl. 30, 714 (1991) as well as lit. cit.
20. H. Bock, U. Stein and A. Semkow, Chem. Ber. 113, 3208 (1980).
21. H. Bock, B. Hierholzer and P. Rittmeyer, Z. Naturforsch. B 44, 187 (1989).
22. Cf. e.g. the review by A.H. Zewail, Scientific American 262, 76 (1990).
23. Cf. e.g. "Structure Correlations" (Eds. H.-B. Bürgi and J.D. Dunitz) Vols. 1 and 2, VCH Verlag, Weinheim 1994.
24. B. Solouki and H. Bock, Inorg. Chem. 16, 665 (1977) and lit. cit.
25. B. Solouki, P. Rosmus and H. Bock, J. Amer. Chem. Soc. 98, 6054 (1976). See also H. Bock, B. Solouki, S. Mohmand, E. Block and L.K. Revelle, JCS Chem. Comm., 287 (1977).

26. H. Bock, T. Hirabayashi and S. Mohmand, Chem. Ber. 115, 492 (1982).
27. E. Block, E.R. Corey, R.E. Penn, T.L. Renken, P.F. Sherwin, H. Bock, T. Hirabayashi, S. Mohmand and B. Solouki, J. Amer. Chem. Soc. 104, 3119 (1981).
28. T. Hirabayashi, S. Mohmand and H. Bock, Chem. Ber. 115, 483 (1982).
29. S. Mohmand and H. Bock, Phosphorus and Sulfur 14, 185 (1983).
30. H. Bock, B. Solouki, G. Bert and P. Rosmus, J. Amer. Chem. Soc. 99, 1663 (1977). Highly correlated Wavefunction $H_2C{=}C{=}S$: P. Rosmus, B. Solouki and H. Bock, Chem. Phys. 22, 453 (1977). For $H_2C{=}C{=}Se$ see H. Bock, S. Aygen, P. Rosmus and B. Solouki, Chem. Ber. 113, 3187 (1980).
31. H. Bock, S. Mohmand, T. Hirabayashi, G. Maier and H.P. Reisenauer, Chem. Ber. 116, 273 (1982).
32. H. Bock, R. Dammel and D. Jaculi, J. Am. Chem. Soc. 108, 7844 (1986).
33. H. Bock, B. Solouki, P. Rosmus, and R. Steudel, Angew. Chem. 85, 987 (1973); Angew. Chem. Int. Ed. Engl. 12, 933 (1973).
34. E. Block, H. Bock, S. Mohmand, P. Rosmus and B. Solouki, Angew. Chem. 88, 380 (1976); Angew. Chem. Int. Ed. Engl. 15, 383 (1976). See also [27].
35. B. Solouki, P. Rosmus and H. Bock, Angew. Chem. 88, 381 (1976); Angew. Chem. Int. Ed. Engl. 15, 384 (1976).
36. M. Binnewies, B. Solouki, H. Bock, R. Becherer and R. Ahlrichs, Angew. Chem. 96, 704 (1984); Angew. Chem. Int. Ed. Engl. 23, 731 (1984).
37. H. Bock, M. Kremer, B. Solouki, M. Binnewies and M. Meisel, J. Chem. Soc. Chem. Commun. 1992, 9.
38. M. Meisel, H. Bock, B. Solouki, and M. Kremer, Angew. Chem. 101, 1378 (1989); Angew. Chem. Int. Ed. Eng. 28, 1373 (1989).
39. H. Bock, M. Kremer, B. Solouki and M. Binnewies, Chem. Ber. 125, 315 (1992).
40. H. Bock, B. Solouki and H.W. Roesky, Inorg. Chem. 24, 4425 (1985) and references quoted therein.
41. O.M. Nefedov, V.A. Korolev, L. Zanathy, B. Solouki and H. Bock, J. Chem. Soc. Mendeleev Commun. 1992, 67 and lit. cit..
42. H. Bock , G. Wagner and J. Kroner, Tetrahedron Lett. 1971, 3713 as well as Chem. Ber. 105, 3850 (1972).

43. H. Bock and G. Brähler, Angew. Chem. 89, 893 (1977); Angew. Chem. Int. Ed. Engl. 16, 855 (1977) as well as Chem. Ber. 112, 3081 (1979).
44. H. Bock, P. Hänel, H.-F. Herrmann and H. tom Dieck, Z. Naturforsch. B 43, 1240 (1988).
45. H. Bock and U. Lechner-Knoblauch, J. Organomet. Chem. 294, 295 (1985).
46. H. Bock, B. Hierholzer and P. Rittmeyer, Z. Naturforsch. B 44, 187 (1988).
47. J. Giordan, H. Bock, M. Eiser and H.W. Roesky, Phosphorus and Sulfur 13, 19 (1982).
48. H. Bock, G. Brähler, U. Henkel, R. Schlecker and D. Seebach, Chem. Ber. 113, 289 (1980).
49. H. Bock, P. Rittmeyer, A. Krebs, K. Schütz, J. Voss and B. Köpke, Phosphorus and Sulfur 19, 131 (1984).
50. H. Bock, P. Rittmeyer, Z. Naturforsch. B 43, 419 (1988) as well as H. Bock, P. Rittmeyer and U. Stein, Chem. Ber. 119, 3766 (1986).
51. H. Bock, B.I. Chenards, P. Rittmeyer and U. Stein, Z. Naturforsch. B 43, 117 (1988).
52. H. Bock, U. Stein, and P. Rittmeyer, Angew. Chem. 94, 540 (1982); Angew. Chem. Int. Ed. Engl. 21, 533 (1982) as well as Angew. Chem. Suppl. 1982 1145-1154.
53. H.Bock, C. Arad, C. Näther and Z. Havlas, unpublished results. Cf. Ph. D. thesis C. Arad, University of Frankfurt 1994, in preparation.
54. H. Bock, A. Rauschenbach, C. Näther and Z. Havlas, unpublished results. Cf. Ph. D. thesis A. Rauschenbach, University of Frankfurt 1994.
55. H. Bock A. Rauschenbach, C. Näther, Z. Havlas A. Gavezzotti and G. Filippini, Angew. Chem. 106 (1994) inprint ; Angew. Chem. Int. Ed. Engl. 3 (1994), inprint.
56. H.Bock, C. Näther, Z. Havlas, A. John and C. Arad, Angew. Chem. 106, 931 (1994); Angew. Chem. Int. Ed. Engl. 33, 875 (1994).
57. Cf. e.g. J. Bernstein "Conformatioanl Polymorphism" in G.R. Desiraju (Ed.) "Organic Solid State Chemistry", Elsevier, Amsterdam 1987, p. 471 f. and references given terein.
58. Cf. e.g. G.R. Desiraju in "Crystal Engeneering", Material Sciece Monographs 54, Elsevier Amsterdam 1989, p. 285 f. and references given therein.